Check for updates

Petasis adducts of tryptanthrin – synthesis, biological activity evaluation and druglikeness assessment†

Pedro Brandão, [ID]‡*[ab] Carolina Marques,‡[b] Eugénia Pinto,[cd] Marta Pineiro[a] and Anthony J. Burke [ID]*[be]

Tryptanthrin is a valuable tetracyclic alkaloid, which displays a wide variety of biological activities. The application of this type of scaffold as a starting material for the discovery of new drug candidates is of major importance in medicinal chemistry. In this work, we report one of the few examples of tryptanthrin-based multicomponent reaction approaches for drug discovery, and the first using the Petasis reaction. The optimized BINOL-catalyzed reaction conditions allowed the synthesis of a library of new tryptanthrin derivatives bearing considerable structural diversity. An asymmetric version was also established, achieving the desired enantiomerically pure derivative with 99% ee and 71% yield. The resulting library was screened against one Gram-positive and one Gram-negative bacteria, two yeasts, and three filamentous and four dermatophyte fungal strains with clinical relevance, with compound 5bea displaying moderate fungicidal activity.

1. Introduction

Diversity-oriented synthesis (DOS) is one of the most effective sources of new small-molecule drug candidates. In medicinal chemistry, it is well-established that library structural diversity, rather than library size, is often a key-point for detecting new biologically active compounds.[1–3] Within DOS, several strategies can be adopted. Multicomponent reactions (MCRs) have emerged as one of the most versatile, efficient, and sustainable avenues to achieve this structural diversity, especially when adapted to drug-discovery settings.[4–6] The opportunity to integrate in a one-step approach three or more reactants in a single chemical framework allows not only the quick preparation of highly substituted libraries, with different substitution patterns, but also contributes to the faster identification of hit

compounds, and even a hit-to-lead optimization process. Using privileged structures as starting components in a MCR approach can therefore be ideal to promote the discovery of new compounds with druglike properties.[7–11]

In 1993, Petasis and Akritopoulou described a new MCR to give allylamines using a secondary amine, paraformaldehyde and (*E*)-vinylboronic acid[12] – a reaction now known as the Petasis borono-Mannich reaction, or simply the Petasis reaction. The reaction has been exhaustively modified over the past 30 years.[13–15] Indeed, in our group we recently applied the Petasis reaction to prepare new 3,3-disubstituted oxindole derivatives using isatin as the starting component.[16] We also reported a new synthetic route employing isatin for the synthesis of the very interesting tetracyclic natural product, tryptanthrin (Fig. 1).[17]

This golden yellow alkaloid (chemically indolo[2,1-*b*]quinazoline-6,12-dione) shows extensive biological activity and has caught the attention of several research groups.[18–20] Indeed, tryptanthrin constitutes an excellent starting point for a polypharmacological approach, as it possesses the ability to interact with multiple targets effectively, namely by modulating the immune system. Several publications have shown its potential as an antibiotic and antiviral agent,[21–25] demonstrating its strong anti-inflammatory and antioxidant activity,[26–33] as well as its anti-allergic action[34,35] and its antiproliferative and antitumoral activity,[36–39] including its anti-angiogenic effect, which is very relevant in the prevention of metastasis.[40,41] The action of tryptanthrin over multiple targets has made it a good candidate for further studies on autoimmune diseases, like

[a] *Department of Chemistry, University of Coimbra, CQC, 3004-535, Coimbra, Portugal. E-mail: pbrandao@qui.uc.pt*

[b] *LAQV-REQUIMTE, University of Évora, Rua Romão Ramalho, 59, 7000-671, Évora, Portugal. E-mail: ajb@uevora.pt*

[c] *Laboratório de Microbiologia, Departamento de Ciências Biológicas, Faculdade de Farmácia, Universidade do Porto, Rua de Jorge Viterbo Ferreira 228, 4050-313 Porto, Portugal*

[d] *CIIMAR—Interdisciplinary Centre of Marine and Environmental Research, Terminal de Cruzeiros do Porto de Leixões, 4450-208 Matosinhos, Portugal*

[e] *Department of Chemistry, University of Évora, Rua Romão Ramalho, 59, 7000-671, Évora, Portugal*

† Electronic supplementary information (ESI) available. See DOI: 10.1039/d1nj02079j

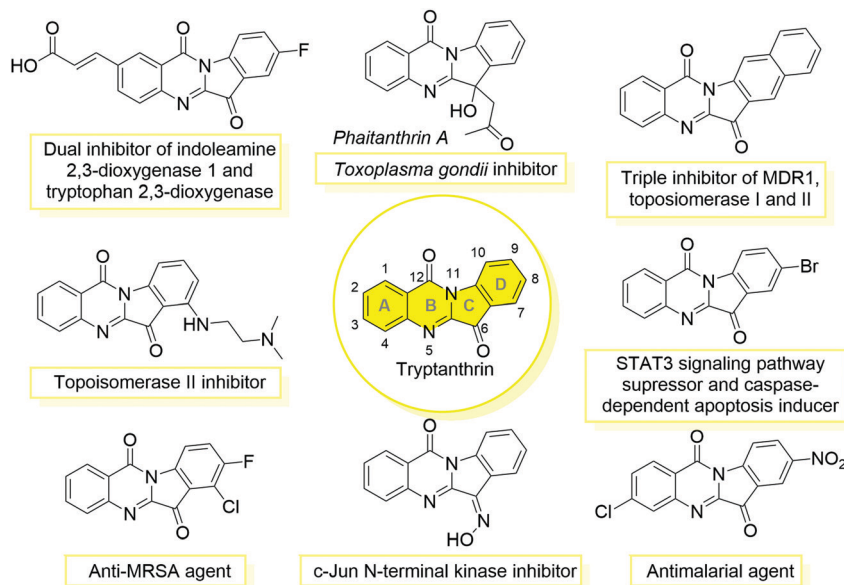‡ These authors contributed equally to this work.

Fig. 1 Tryptanthrin and derivatives with diverse biological activities.

psoriasis[42] and rheumatoid arthritis.[43] Moreover, this molecule presents a favorable pharmacokinetic profile as it is able to reach multiple target organs, including the central nervous system, by crossing the blood–brain barrier (BBB). The fact that it is orally bioavailable and is not subject to P-glycoprotein efflux makes it a great candidate for further studies.[44,45] Several tryptanthrin derivatives are shown in Fig. 1, and some have been reported with antitumor,[46–55] anti-inflammatory,[56] antitubercular,[57] antiparasitic,[58–60] and antibacterial/antifungal activities,[52,61] as well as being anti-phytopathogenic agents (including viruses and fungi).[62]

There are few reports on the use of tryptanthrin in MCRs, one example being the Knoevenagel-initiated multicomponent reaction between tryptanthrin, malononitrile and different C–H-activated carbonyl compounds in the presence of ammonium acetate.[63] In this report we present the first tryptanthrin-based Petasis MCR, and the study of the antifungal and antibacterial effects of tryptanthrin derivatives. Conscious of the important role

that MCRs[64–67] and chiral molecules play in the drug-discovery process,[68–70] we have developed an asymmetric route to enantiopure tryptanthrin-based Petasis adducts.

2. Results and discussion

2.1. Chemistry

Synthesis of tryptanthrin derivatives and the corresponding borylated derivatives. The synthesis of brominated tryptanthrins was achieved using the classic condensation between (un)substituted isatins and (un)substituted isatoic anhydrides in the presence of a base, adapting procedures previously reported in the literature for the synthesis of these brominated tetracycles.[48,59,71] We selected potassium carbonate as the base and allowed the reaction to proceed overnight in DMF at room temperature. Four brominated tryptanthrin derivatives, **1a–d**, were isolated and they were used in the next step without the
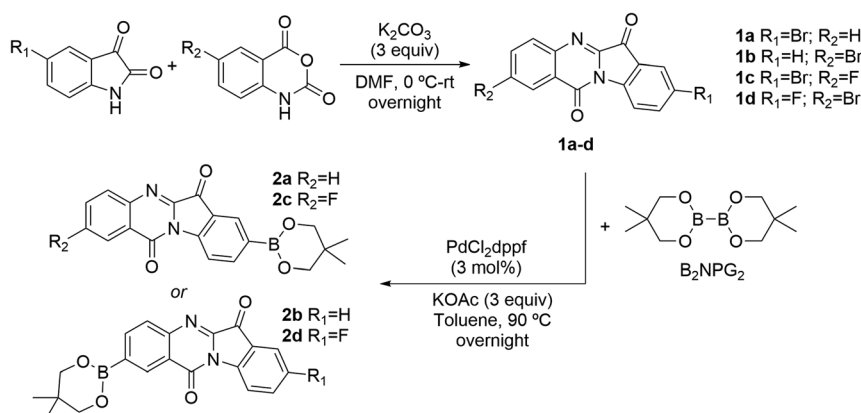
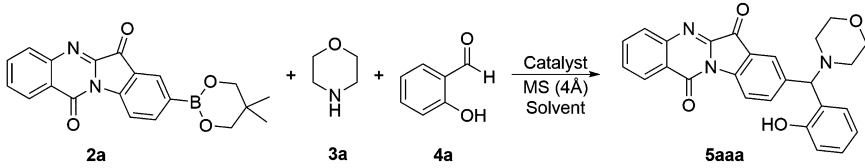Scheme 1 Tryptanthrin synthesis from isatin and consecutive borylation.

need for further purification (74–95% yield). The brominated tryptanthrin derivatives were then borylated with B_2NPG_2 in the presence of $PdCl_2(dppf)$ and KOAc in toluene. The reaction was carried out at 90 °C overnight. At this stage, we verified that tryptanthrins **1a–d** were successfully borylated in high yields without the requirement of tedious work-up procedures (80% to quantitative yield). The overall synthetic pathway is shown in Scheme 1.

Three-component Petasis reaction. The Petasis reaction was fully optimized by studying different solvents, catalysts and temperatures. Borylated tryptanthrin **2a**, morpholine **3a** and salicylaldehyde **4a** were selected for the model reaction, and the optimization is depicted in Table 1. Several different non-polar, polar aprotic and polar protic solvents were evaluated, especially those typically employed in the Petasis reaction, including benzotrifluoride,[72] which is a green substitute for dichloromethane. Although acetonitrile and 1,2-dichloroethane exhibited slightly higher yields than chloroform, we chose the latter as it allowed a more straightforward work-up, a lower operating temperature, and the components showed superior solubilities, even at room temperature. With this in mind, to improve the reactivity, we decided to screen different metal-based catalysts and organocatalysts. First, the literature method using CuBr/bpy was used (Table 1, entry 8) but it failed to give the desired product.[73] Lewis acids were also screened in the Petasis reaction[74] (for example, $Fe(OTf)_2$, $Yb(OTf)_3$ and $InCl_3$ – Table 1, entries 9–11) but failed to improve the yield above that of the catalyst-free reaction. Moreover, N,N'-diphenylthiourea (DPTU) allowed only a modest improvement in the yield (Table 1, entry 12). Gratifyingly, (±)-BINOL proved to be the most efficient catalyst (Table 1, entry 13), giving the highest yield of 66%.

After finding the ideal conditions, we next studied a variety of different substrates (Fig. 2). Besides the four already described borylated tryptanthrins **2a–2d**, several secondary amines (cyclic, aliphatic and disubstituted amines **3a–3k**) and aldehydes (salicylaldehyde **4a**, salicylaldehyde derivatives **4b–4i**, benzaldehyde **4j**, glyoxylic acid **4k**, and propanal **4l**) were tested. We verified that the four borylated tryptanthrins were successfully converted to the corresponding Petasis products. With this approach, we verified that borylation is only selective for the Br unit, with no borylation occurring at the fluorine position. Furthermore, in agreement with the literature precedent[16] the multicomponent BINOL-catalyzed reaction is successful when *ortho*-hydroxybenzaldehydes are used, as the reaction does not proceed with other aldehydes **4j–4l**. In the case of amines, cyclic secondary amines (except for **3b**), and *N*-substituted benzylamine **3e** could be successfully used, whereas aromatic amines **3f** and **3g**, and aliphatic amines **3h–3k** failed to afford any products. We also noticed that, in most cases, higher yields were observed when the reaction occurred at position 2 of the tryptanthrin unit, as opposed to reaction at position 8, except for aldehyde **4d** and aldehyde **4c**, which gave higher yields. Furthermore, the yields were lower with the fluorine-containing tryptanthrin substrates, probably due to some form of deactivating effect. A library of 20 novel tryptanthrin derivatives was obtained using the Petasis multicomponent reaction. The yields were quite variable (10–80%) (Scheme 2).

Asymmetric Petasis reaction. Motivated by the results obtained for the synthesis of the library of tryptanthrin-based Petasis adducts, we decided to look at the asymmetric version. The natural choice of catalyst based on our studies (Table 2) was BINOL.[75,76] In addition, we also looked at two other chiral

Table 1 Optimization of the Petasis reaction conditions

Entry[a]	Catalyst	Solvent	Temperature (°C)	Time (h)	Yield[b] (%)
1	—	CHCl$_3$	70	24	24
2	—	Toluene	90	15	14
3	—	BTF	110	24	<10
4	—	CH$_2$Cl$_2$	50	24	0
5	—	MeOH	90	24	10
6	—	CH$_3$CN	90	24	36
7	—	DCE	90	24	38
8	CuBr/bpy	DMF	70	36	0
9	Fe(OTf)$_2$	CHCl$_3$	70	24	22
10	Yb(OTf)$_3$	CHCl$_3$	70	24	23
11	InCl$_3$	CHCl$_3$	70	24	22
12	DPTU	CHCl$_3$	70	24	31
13	BINOL	CHCl$_3$	70	24	66

[a] Reaction conditions: **2a** (0.3 mmol), **3a** (1.1 mmol), **4a** (0.9 mmol), catalyst (20 mol%), MS 4 Å (200 mg) and solvent (3 mL) were added to a Radley's® 12-position carousel reactor tube under a nitrogen atmosphere and stirred at the indicated temperature for a certain time. [b] Isolated yield. BTF = benzotrifluoride. DPTU = N,N'-diphenylthiourea. BINOL = (±)-1,1′-bi-2-naphthalene-2,2′-diol. bpy = 2,2′-bipyridyl, DCE = 1,2-dichloroethane.
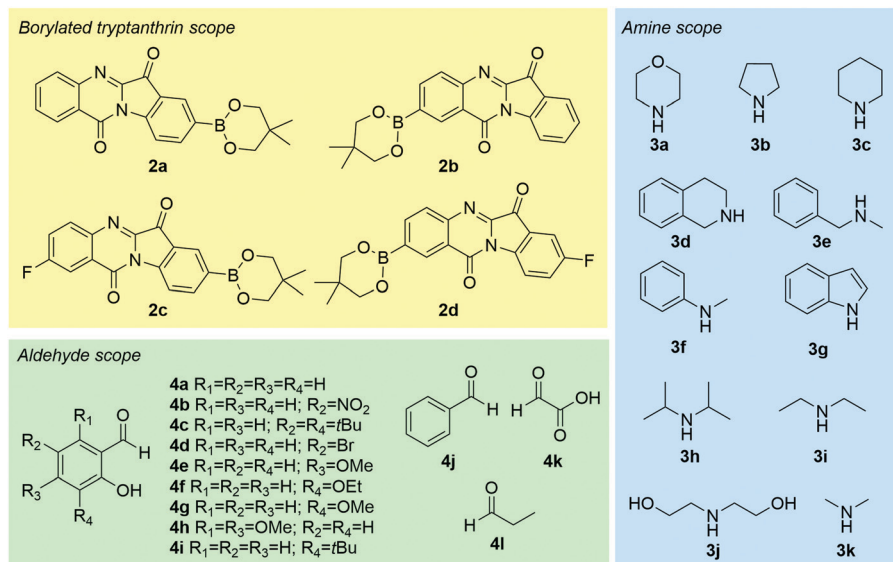
Fig. 2 Reagent scope for the Petasis multicomponent reaction.

diols, namely diisopropyl tartrate (DT) and 2,3-dimethoxy-2,3-dimethyl-5,6-bis(hydroxymethyl) dioxane (diolane), as well as the BINOL phosphoric acid derivative (R)-BNPPA (Table 2, entry 2), the disulfoxide derivative (M,S,S)-p-Tol-BINASO (Table 2, entry 3),[77] and the hydroxyl-bearing alkaloids (+)-cinchonine (Table 2, entry 6) and (−)-quinine (Table 2, entry 7).

A remarkable enantioselectivity of 99% was achieved using (R)-BINOL (Table 2, entry 1). The stereochemical configuration was assigned as S based on the literature precedent.[16,78,79] We then proposed the mechanistic pathway depicted in Scheme 3. We presume that after rapid generation of an iminium intermediate from nucleophilic addition of **3a** and **4a** (molecular sieves promote this reaction, capturing the water formed in this step), this ion is attacked by the *in situ*-generated BINOL-boronic ester on the Re-face of the iminium intermediate, leading to the final product with S-configuration. BINOL is then presumably recovered by hydrolysis.

Significant enantioselectivities were also observed with diisopropyl tartrate (DT) (Table 2, entry 4, 86% ee) and diolane (Table 2, entry 5, 59% ee). All the other catalysts tested gave almost no enantioselectivity. This indicated that diol-containing catalysts were the most effective in the Petasis reaction. On reducing the amount of morpholine and salicylaldehyde in the reaction we noticed a drop in both the yield and the enantioselectivity (Table 2, entry 8).

After defining our synthetic strategy to obtain both racemic and enantiomerically enriched products our next task was an evaluation of their pharmacological properties.

## 2.2. Druglikeness evaluation

The determination of different physico-chemical properties of drug candidates, as well as their pharmacokinetic profiles, is often a time-consuming task. Luckily, several tools have been developed recently to perform, *in silico*, the pre-evaluation of these properties for new molecules, such as ADME-space,[80] ADMETlab,[81] DRUDIT,[82] and SwissADME.[83] We selected the latter for screening our tryptanthrin derivatives, as it is a web-based free tool that is easy to use and which provides a wide range of results. Furthermore, SwissADME also evaluates the compliance of small-molecules with druglikeness rules/filters that are routinely applied by the pharmaceutical industry and academic research groups for the selection of compounds, *i.e.* – the Lipinski (Pfizer) rule of five,[84,85] Ghose (Amgen) filter,[86] Veber (GSK) filter,[87] Egan (Pharmacopeia) filter,[88] and Muegge (Bayer) filter.[89]

Some of the relevant structural features evaluated by these filters are the number of hydrogen-bond acceptors and donors, and the number of rotatable bonds (Fig. 3). Gratifyingly, all our compounds were found to be within the established limits of these rules.

This versatile tool allows the prediction and calculation of several other physico-chemical molecular properties that are of relevance to their druglikeness and inherent pharmacokinetic profiles, such as molecular weight (M_W), calculated partition coefficient (clog P), molar refractivity (M_R), topological polar surface area (TPSA), and water solubility (log S). Table 3 summarizes these data.
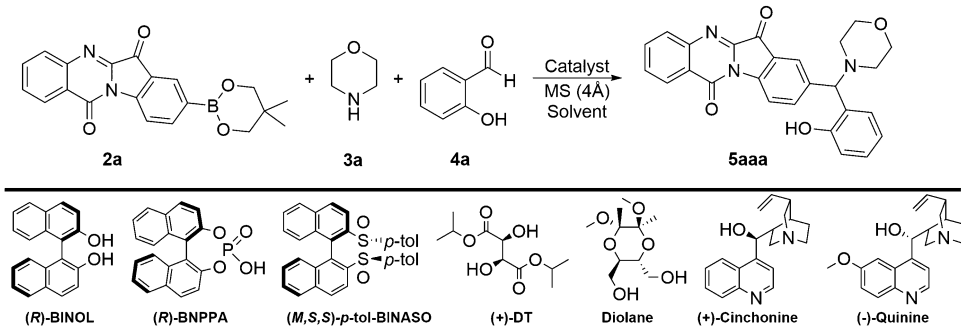
Analysis of these results led to the following conclusions. Starting with M_W, this property is considered in the Lipinski ($M_W \leq 500$ Da), the Ghose ($160 \leq M_W \leq 480$ Da), and the Muegge rules ($200 \leq M_W \leq 600$ Da). Our library spanned the range $437.49 \leq M_W \leq 551.68$ Da, meaning that, unfortunately, six of these new compounds do not comply with the Lipinski rule, although it is also known that compounds that violate one of the Lipinski rules can still be compliant with the Lipinski filter and even end up as a successful drug. All the compounds fall within the scope of the Muegge filter, but several of these compounds do not comply with the parameterization established by the Ghose filter. M_R is taken into consideration only by the Ghose filter ($40 \leq M_R \leq 130$), and our compounds spanned the
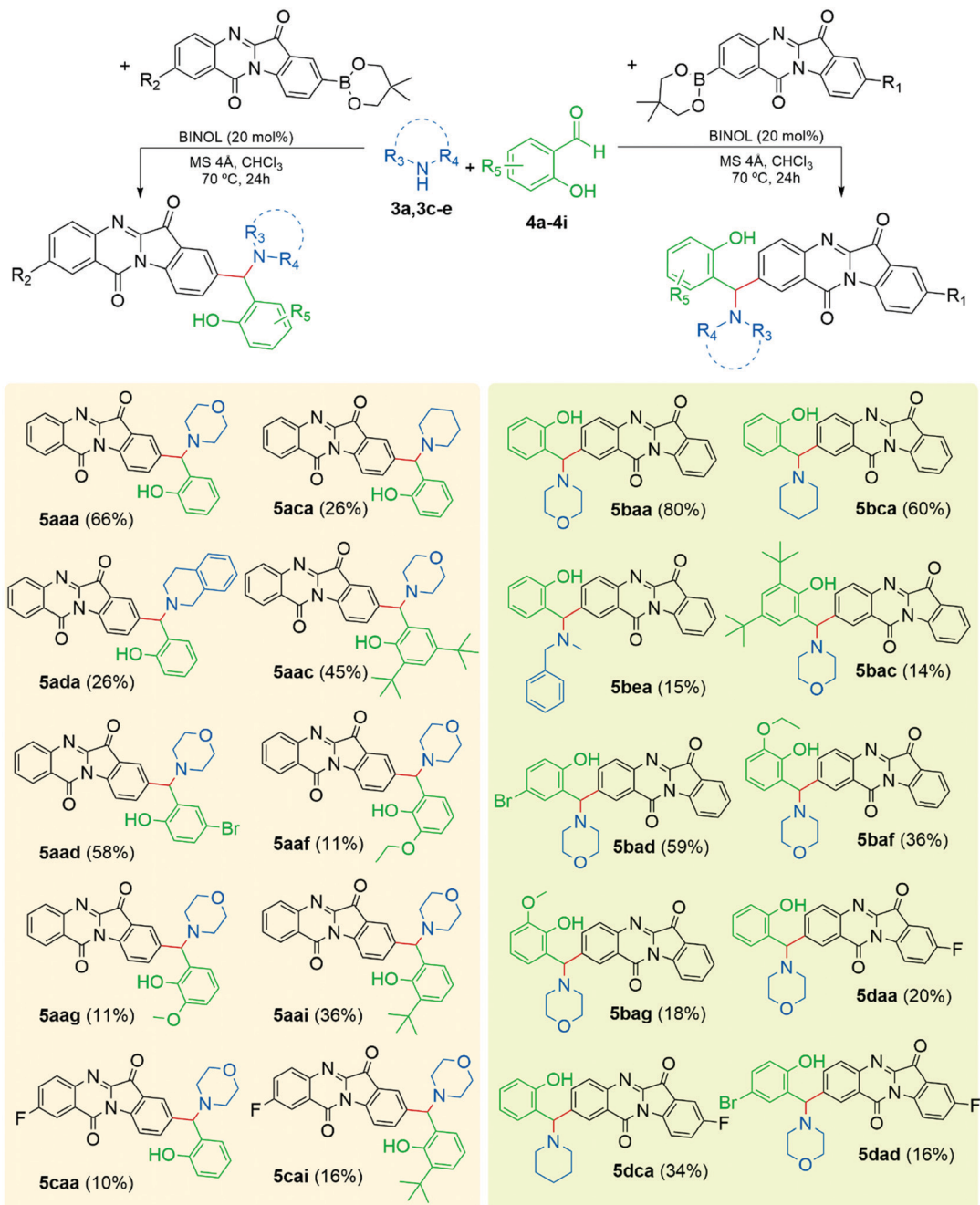
Scheme 2 Library of tryptanthrin derivatives obtained *via* the Petasis MCR.

interval $127.22 \leq M_R \leq 165.80$, meaning that several of them are beyond the upper limit of this filter. The TPSA is evaluated in the Veber filter (TPSA ≤ 140 Å^2), the Egan filter (TPSA ≤ 131.6 Å^2), and the Muegge filter (TPSA ≤ 150 Å^2). The 20 compounds possess calculated TPSAs between 75.43 Å^2 and 93.89 Å^2, and therefore are compliant with these rules in this respect. Lipophilicity is a very relevant feature for any new drug, a property that will determine several aspects of its pharmacokinetic behavior, especially absorption and distribution, as it will allow the molecule to cross membranes and be distributed across different tissues with different extensions and rates. Hence, clog P

is one of the most important properties to be evaluated for new drug candidates, and thus is considered by four of the five filters evaluated – the Lipinski filter (clog $P \leq 5$), Ghose filter ($-0.4 \leq$ clog $P \leq 5.6$), Egan filter (clog $P \leq 5.88$), and Muegge filter ($-2 \leq$ clog $P \leq 5$). The synthesized library exhibited clog P values in the range of 2.78 to 5.23, meaning that all the compounds are in compliance with the Ghose and Egan filters, and only two compounds (**5aac** and **5bac**) have values that are slightly above the upper limit of the Lipinski and Muegge filters. This is probably due to the presence of two *tert*-butyl groups, which significantly increases the lipophilicity of these two compounds.

Table 2   Asymmetric Petasis 3-MCR using borylated tryptanthrin (**2a**), morpholine (**3a**) and salicylaldehyde (**4a**)

Entry[a]	Catalyst	Yield[b] (%)	ee[c] (%)
1	(*R*)-BINOL	71	99
2	(*R*)-BNPPA	41	<10
3	(*M,S,S*)-*p*-Tol-BINASO	32	<5
4	L-(+)-DT	40	86[e]
5	Diolane	32	59[e]
6	(+)-Cinchonine	42	<5
7	(−)-Quinine	29	<5
8[d]	(*R*)-BINOL	53	75

[a] Reaction conditions: **2a** (0.3 mmol), **3a** (1.1 mmol), **4a** (0.9 mmol), catalyst (20 mol%), MS 4 Å (200 mg) and CHCl$_3$ (3 mL) were added to a Radley's® 12-position carousel reactor tube under a nitrogen atmosphere and stirred at 70 °C for 24 h. [b] Isolated yield. [c] Determined using chiral HPLC (see ESI for further details). [d] Reaction performed with 1.2 equiv. of (**3a**) and 1.2 equiv. of (**4a**). [e] The major enantiomer has the (*R*)-configuration.
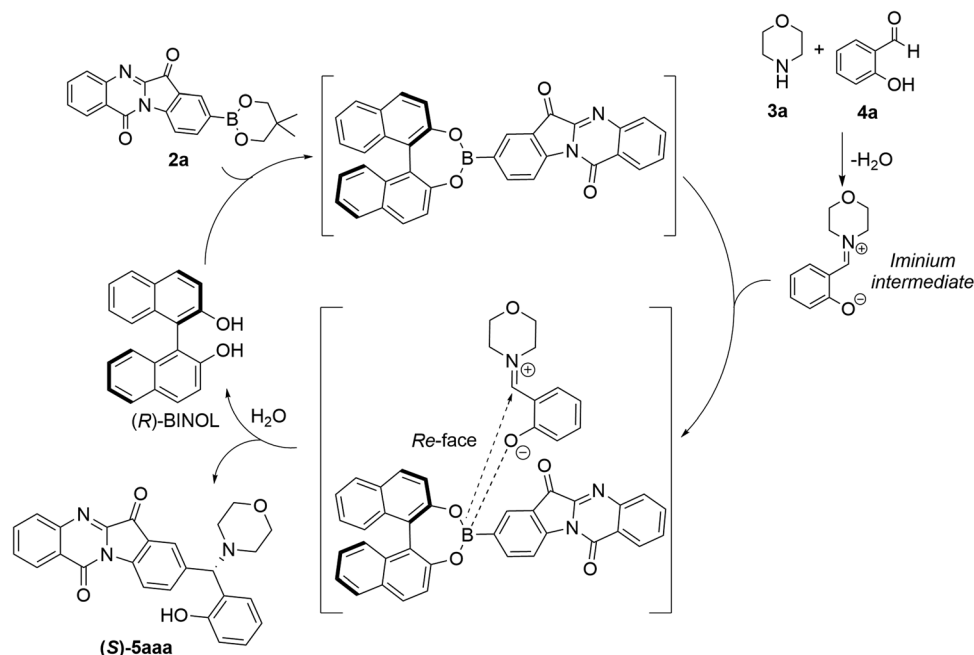

Scheme 3   Proposed mechanism for the (*R*)-BINOL-catalyzed asymmetric reaction.

Fig. 4 depicts the correlation of clog *P* and M_W for these compounds, as well as the upper limits imposed by the different filters, as the correlation between these two parameters is often a good indicator of druglikeness and leadlikeness of the compounds.

The water solubility of new drug candidates, although it is not taken in consideration directly in any of the five filters, is an important feature. Highly water-soluble molecules are not able to cross the bilipid plasma membrane and therefore routes of administration other than intravenously might be limited or be dependent on active transport. Poorly water-soluble molecules might face problems in their distribution, and most likely will need to bind to serum albumin to be carried in the bloodstream.
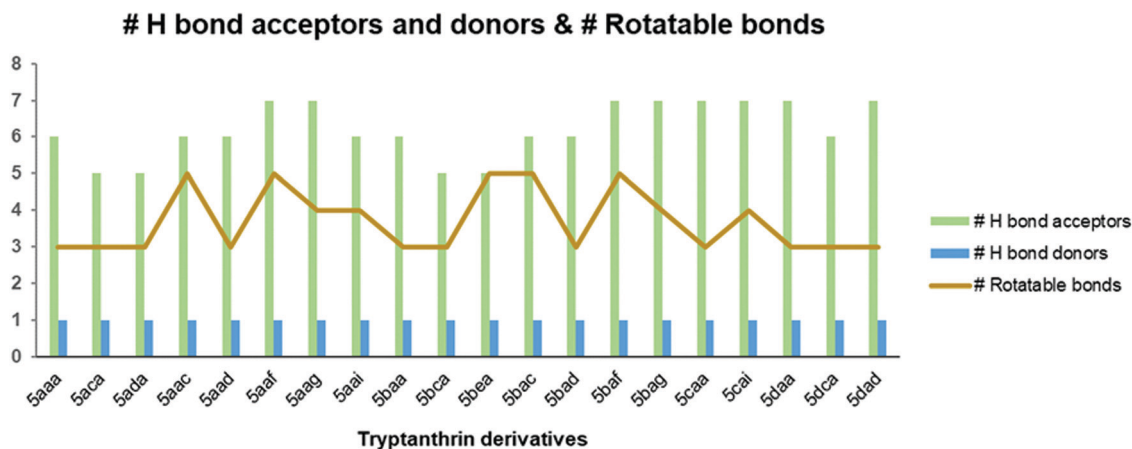
Fig. 3 Calculated hydrogen-bond acceptors, hydrogen-bond donors, and rotatable bonds for our library.

Table 3 *In silico* calculation of several physical–chemical properties of the synthesized tryptanthrin derivatives

Compounds	M_W (Da)	M_R	TPSA[a] ($Å^2$)	$\text{clog} P$[b]	$\log S$[c]
5aaa	439.46	127.26	84.66	2.79	−4.29
5aca	437.49	130.98	75.43	3.65	−5.36
5ada	485.53	146.01	75.43	4.20	−6.07
5aac	551.68	165.80	84.66	5.13	−7.76
5aad	518.36	134.96	84.66	3.34	−5.00
5aaf	483.52	138.56	93.89	3.10	−4.83
5aag	469.49	133.75	93.89	2.78	−4.45
5aai	495.57	146.53	84.66	3.97	−6.03
5baa	439.46	127.26	84.66	2.87	−4.29
5bca	437.49	130.98	75.43	3.73	−5.36
5bea	473.52	139.25	75.43	4.21	−6.03
5bac	551.68	165.80	84.66	5.23	−7.76
5bad	518.36	134.96	84.66	3.49	−5.00
5baf	483.52	138.56	93.89	3.19	−4.83
5bag	469.49	133.75	93.89	2.85	−4.45
5caa	457.45	127.22	84.66	3.09	−4.45
5cai	513.56	146.49	84.66	4.27	−6.13
5daa	457.45	127.22	84.66	3.17	−4.39
5dca	455.48	130.94	75.43	4.04	−5.46
5dad	536.35	134.92	84.66	3.79	−5.12

[a] Calculated in accordance with ref. 90 [b] SwissADME provides 5 $\log P$ values, calculated according to different methodologies, and an average value of these calculations (shown in the table). [c] Calculated in accordance with ref. 91 M_W = molecular weight. M_R = molar refractivity. TPSA = topological polar surface area. $\text{clog} P$ = calculated partition coefficient. $\log S$ = water solubility.

Most orally administered small-molecule drugs, as organic molecules, possess moderate to poor water solubility. Prodrugs and different formulations often allow the improvement of the solubility of the drugs, assuring that they reach their final target. All the compounds evaluated possess a $\log S$ between −7.76 and −4.29, and are classified as poorly soluble ($-10 \leq \log S \leq -6$) or moderately soluble ($-6 \leq \log S \leq -4$).

Another advantageous feature of the SwissADME tool is that it provides a BOILED-Egg (Brain Or IntestinaL EstimateD permeation method) model, which predicts the potential of these drug-like compounds to cross the gastrointestinal barrier *via* passive diffusion and therefore making them good candidates for administration *per os* (white area) as well as the
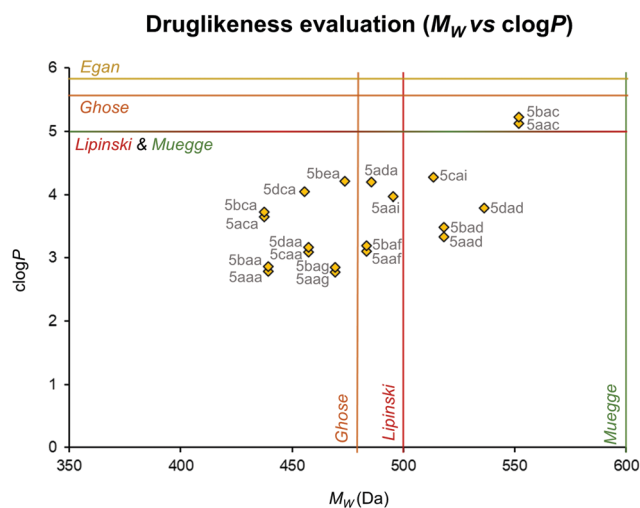

Fig. 4 Relationship between M_W and $\text{clog} P$ of the synthesized compounds and their placement according to the upper limits of the main filters.

blood–brain barrier (BBB) (yolk/yellow area).[92] This model correlates the TPSA with the lipophilicity displayed by these compounds (the term $W \log P$ is used, calculated according to the methodology established by Wildman and Crippen[93]). Fig. 5 shows where the synthesized compounds are placed in this model. Interestingly, four compounds (**5dca**, **5ada**, **5aca**, and **5bca**) presented features that make them suitable for BBB permeation, which might be relevant for further studies involving this family of compounds. Upon detailed analysis of their structures, we can infer that those compounds containing a piperidine or 1,2,3,4-tetrahydroisoquinoline appendage as the secondary amine component have a lower TPSA. The remaining derivatives are placed in the "egg white" area, and therefore can potentially be the subject of passive gastrointestinal absorption, making them good candidates for oral drug administration.

Another interesting feature evaluated by the SwissADME tool is the presence or absence of Pan-Assay Interference
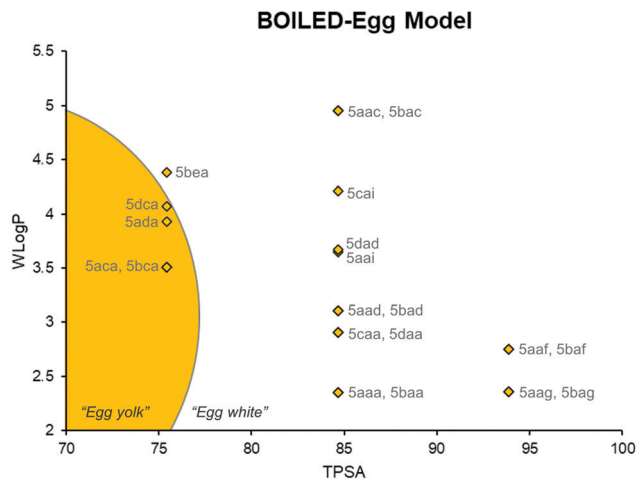
BOILED-Egg Model

Fig. 5 BOILED-Egg model for the tryptanthrin derivatives obtained *via* Petasis MCRs.

Compounds (PAINS), compounds that interact with multiple targets (promiscuous compounds), and therefore often are identified as hit compounds towards a certain target, although their potential as future drug candidates is compromised by their potential to exert off-target effects.[94,95] All our compounds contain a phenolic Mannich base unit, which is described as a possible PAINS fragment. Although this can constitute a drawback for the drug development of these molecules, it is important to understand that several compounds bearing this structural feature exhibit significant bioactivity and therefore early removal from the drug-discovery pipeline might be a mistake.[96] An example is the drug lurbinectedin (commercialized as Zepzelca), which was granted accelerated approval by the FDA in 2020 for the treatment of metastatic small cell lung cancer and bears a phenolic Mannich base in its structure.[97,98] Furthermore, a recent study has indicated that the removal of potential-PAINS compounds from the drug-discovery pipeline needs to be based on more than the presence of these substructures, as their PAINS activity is highly dependent on the overall molecular structure.[99] With this in mind, more studies will need to be conducted in order to verify whether or not the phenolic Mannich bases displayed by this new library will determine their fate in the drug-discovery pipeline.

Table 4 indicates the overall compliance of the synthesized compounds with the five druglikeness filters.

All the novel tryptanthrin derivatives comply with the Lipinski, Veber, and Egan filters. With the Muegge filter, only compounds **5aac** and **5bac** are non-compliant, due to their high lipophilicity, to which the two *tert*-butyl substituents in the phenol moiety have a major contribution. Compliance with the Ghose filter is only observed with compounds **5aaa**, **5baa**, **5caa**, and **5daa**. The violations of the Ghose filter are mostly due to the high M_R values (16 compounds), followed by the high M_W values (10 compounds) and, for compounds **5aac** and **5bac** that display three violations of the Ghose filter, the compounds are in violation of the third rule, which is that the number of atoms should be below 70. The overall scores showcase a good druglikeness for all the newly described tryptanthrin derivatives, moreover even in the case of those compounds that are non-compliant with the Muegge (**5aac** and **5bac**) and Ghose filters (**5aca**, **5ada**, **5aac**, **5aad**, **5aaf**, **5aag**, **5aai**, **5bca**, **5bea**, **5bac**, **5bad**, **5baf**, **5bag**, **5cai**, **5dca**, and **5dad**), the values are just outside the upper limits. The *in silico*-evaluated physico-chemical properties, as well as the BOILED-Egg model, showcase the potential for these molecules to be further screened for several possible druggable targets.

2.3. Antimicrobial activity evaluation

The antifungal activity was evaluated against nine fungal strains: two yeasts (*Candida albicans* and *Candida krusei*); three filamentous fungi (*Aspergillus fumigatus*, *Aspergillus niger*, and *Mucor* spp.); and four dermatophyte species (*Trichophyton rubrum*, *Trichophyton mentagrophytes*, *Microsporum canis*, and *Nannizzia gypsea*). The antibacterial activity was evaluated against *Escherichia coli* and *Staphylococcus aureus*.

The minimum inhibitory concentrations (MICs) and minimal lethal concentrations (MLCs) were used for defining the antimicrobial activity, in agreement with the references of the Clinical and Laboratory Standards Institute (CLSI).[100] The MIC was determined as the lowest concentration resulting in 100% growth inhibition, in comparison with the sample-free control, and the MLC was defined as the lowest concentration at which no colonies grew after incubation.

The library of 20 tryptanthrin derivatives, as well as the enantiomerically pure version of **5aaa**, did not display any antibacterial activity against the two bacterial strains tested, at 512 µg mL^{-1}.

The antifungal susceptibility testing results showed that the synthesized compounds do not exhibit relevant antifungal

Table 4 Druglikeness filter compliance for the 20 tryptanthrin derivatives obtained *via* Petasis MCRs (the number indicates the number of rules breached)

		Tryptanthrin derivatives																		
		5aaa	**5aca**	**5ada**	**5aac**	**5aad**	**5aaf**	**5aag**	**5aai**	**5baa**	**5bca**	**5bea**	**5bac**	**5bad**	**5baf**	**5bag**	**5caa**	**5cai**	**5daa**	**5dca**	**5dad**
Filters	Lipinski	0	0	0	0	0	0	0	0	0	0	0	0	0	0	0	0	0	0	0	0
	Ghose	0	**1**	**2**	**3**	**2**	**2**	**1**	**2**	0	**1**	**1**	**3**	**2**	**2**	**1**	0	**2**	0	**1**	**2**
	Veber	0	0	0	0	0	0	0	0	0	0	0	0	0	0	0	0	0	0	0	0
	Egan	0	0	0	0	0	0	0	0	0	0	0	0	0	0	0	0	0	0	0	0
	Muegge	0	0	0	**1**	0	0	0	0	0	0	**1**	0	0	0	0	0	0	0	0	0

Note: A score of 0 stipulates a compliance with the filter, while a bold score > 0 means the compounds do not comply with the designated filter.

Table 5 Antifungal activity (MIC and MLC) of the tryptanthrin derivatives for dermatophyte fungal strains

| Compound | MIC[a]/MLC[b] (μg mL^{-1}) | | | |
	Trichophyton mentagrophytes	Trichophyton rubrum	Microsporum canis	Nannizzia gypsea
5aaa	>512/>512	>512/>512	>512/>512	>512/>512
5aca	>512/>512	>512/>512	>512/>512	>512/>512
5ada	>512/>512	>512/>512	>512/>512	>512/>512
5aac	256/256	256/>512	256/>512	512/>512
5aad	>512/>512	>512/>512	>512/>512	>512/>512
5aaf	>512/>512	>512/>512	>512/>512	>512/>512
5aag	>512/>512	>512/>512	>512/>512	>512/>512
5aai	>512/>512	>512/>512	>512/>512	>512/>512
5baa	>512/>512	>512/>512	>512/>512	>512/>512
5bca	256/>512	512/>512	512/>512	>512/>512
5bea	64/64	64/128	64/64	256/>512
5bac	512/512	256/>512	512/>512	>512/>512
5bad	>512/>512	>512/>512	>512/>512	>512/>512
5baf	>512/>512	>512/>512	>512/>512	>512/>512
5bag	>512/>512	>512/>512	>512/>512	>512/>512
5caa	>512/>512	>512/>512	>512/>512	>512/>512
5cai	>512/>512	>512/>512	>512/>512	>512/>512
5daa	>512/>512	>512/>512	>512/>512	>512/>512
5dca	>512/>512	>512/>512	>512/>512	>512/>512
5dad	>512/>512	>512/>512	>512/>512	>512/>512
(S)-5aaa[c]	>512/>512	>512/>512	>512/>512	>512/>512

[a] MIC = minimum inhibitory concentration. [b] MLC = minimum lethal concentration. [c] Enantiomerically pure compound, resulting from the asymmetric catalytic synthesis of compound **5aaa**.

activity against either the tested *Candida* strains or the filamentous fungi, *Aspergillus* and *Mucor* strains, evaluated. More promising results were observed when screening the library against dermatophyte fungi (Table 5). These findings are relevant, as dermatophytes are responsible for many infectious clinical manifestations, especially skin infections, in both humans and animals. Furthermore, these pathogens can be extremely difficult to eliminate, as they exhibit several resistance mechanisms against current therapeutic options.[101,102]

Compound **5bea** displayed the most promising results, with moderate activity against the four dermatophytes tested. The best results were obtained against *T. mentagrophytes* and *M. canis*, with MIC/MLC values of 64 μg mL^{-1}, and *T. rubrum*, with MIC/MLC values of 64/128 μg mL^{-1}. This indicates that, against these three strains, this compound possesses fungicidal activity. This compound was also the most active against *N. gypsea*, but with weak activity (256 μg mL^{-1} MIC value and 512 μg mL^{-1} MLC value). Compounds **5bac**, **5bac**, and **5bca** also displayed weak antifungal activity against these four dermatophytes, in most cases with a fungistatic effect. Noteworthy is also the fact that the results achieved with the racemic mixture **5aaa** and (S)-**5aaa** were identical. Overall, these findings indicate that our compounds showed some degree of selectivity, particularly **5bea**, towards dermatophyte fungal infections.

Structurally, these findings provide important information for future drug development and hit-to-lead optimization. One piece of information that stands out is that the only example of an acyclic secondary amine translated into the most active compound against dermatophyte fungal strains. Those compounds based on the aldehyde **4c** unit showed activity, regardless of the structure of the tryptanthrin ring (compounds **5aac** and **5bac**). The presence of two *tert*-butyl groups also seems to be conducive to biological activity, as compounds bearing only one *tert*-butyl group

(**5aai** and **5cai**) do not display antifungal activity. By comparing compounds **5bca** and **5aca**, we saw that the location of the MCR-formed benzylamine moiety on the tryptanthrin ring has a bearing on the biological activity, since **5bca** possesses some antifungal activity, and **5aca** none. Comparing compounds **5bea** and **5ada**, we can also hypothesize that using less rigid benzylamines as the starting material (**3e** *versus* the rigid **3d**) is crucial for the antifungal activity observed.

Integrating the knowledge obtained from the druglikeness evaluation and the antifungal studies, we observe that the most active compound (**5bea**) complies with all five rules. Compounds **5aac** and **5bac**, despite being the least compliant against the druglikeness filters, can still be considered for further studies, as dermatophyte fungal infections usually only require local/topical treatment, and therefore systemic pharmacokinetic behavior/oral bioavailability is not a crucial parameter to take into consideration. Taking a closer look at Fig. 4 and 5, we can also infer that there appears to exist a correlation between the log$P$ value displayed by these new tryptanthrin derivatives and their antifungal activities, with the most active compounds being amongst those with higher log$P$ values.

3. Conclusions

The Petasis MCR was successfully used for the synthesis of a library of novel tryptanthrin derivatives, allowing high structural diversity in both the quinolone and isatin moieties of tryptanthrin in a simple and efficient one-pot procedure. The full synthetic process is also very efficient, as the synthesis of tryptanthrin and the corresponding borylated derivatives is virtually quantitative and does not require expensive and

tedious work-up procedures. This work is one of the few examples found in the literature on the combination of MCRs with the tryptanthrin scaffold, and the first one using the Petasis MCR. Furthermore, a successful asymmetric version of this valuable chemical transformation is also reported, with (R)-BINOL giving the best results. The bioactivity screening performed indicates compound **5bea** as the most promising and selective compound against dermatophyte fungal strains. As this compound possesses moderate fungicidal activity against *T. mentagrophytes*, *T. rubrum* and *M. canis* it should be a good starting point for developing new antifungal agents. *In silico* evaluation of the physico-chemical properties of the synthesized library also indicates the relevance of $\log P$ and the inclusion of flexible benzylamine moieties, which could be valuable data for the further oriented synthesis of novel antifungal tryptanthrin-based drug candidates.

4. Experimental section

4.1. Chemistry

Reagents were obtained from Sigma-Aldrich, Acros, Strem and Alfa Aesar and were used as received. The solvents used were dried using current laboratory techniques.[103] Borylation reactions and Petasis reactions were conducted in a Radley's® 12-position carousel reactor under a nitrogen atmosphere or in round-bottom flasks. The 4 Å molecular sieves (1–2 mm, 0.04–0.08 in) were obtained from Alfa Aesar (used as received). Column chromatography was carried out on silica gel for flash chromatography (Carlo Erba, 40–63 μm, 60 Å). Thin-layer chromatography (TLC) was carried out on aluminum-backed Kieselgel 60 F254 plates (Merck and Machery Nagel). Plates were visualized either by UV light or with phosphomolybdic acid in ethanol. Melting point (m.p.) values were determined using Barnstead Electrothermal 9100 apparatus and are uncorrected. NMR spectra were recorded using a Bruker Avance III instrument (400 MHz). Chemical shifts (δ) are quoted in parts per million (ppm) with respect to the solvent (CDCl$_3$, ^{1}H: δ = 7.26 ppm, ^{13}C: δ = 77.2 ppm; [d_6]DMSO, ^{1}H: δ = 2.50 ppm, ^{13}C: δ = 39.5 ppm). Coupling constants (J) are reported in Hz and refer to apparent peak multiplicities. Splitting patterns are reported as s, singlet; d, doublet; dd, doublet of doublets; t, triplet; q, quadruplet; m, multiplet; br, broad. Mass spectra (MS) were recorded using a Waters ZQ4000 quadrupole mass spectrometer. The ionization was performed by ESI (Electrospray ionization) and the samples were infused in methanol. High-performance liquid chromatography (HPLC) analysis was carried out using a Hitachi Primaide instrument, equipped with a 1410 series UV detector. A Daicel Chiralpak IA column was used as the stationary phase, with *n*-hexane/ethanol as the mobile phase and 254 nm was used as the wavelength in the UV light detector.

4.1.1. General procedure for the synthesis of tryptanthrin derivatives (1a–d). In a round-bottom flask placed in an ice bath, (un)substituted isatin (1 equiv.) was dissolved in DMF (20 mL). Potassium carbonate (3 equiv.) was slowly added, and allowed to stir, leading to a colour change and hydrogen release. Once the gas production had ceased, the suspension was kept at room temperature and (un)substituted isatoic anhydride (1.2 equiv.) was added. The reaction was allowed to proceed overnight, with stirring at room temperature and monitored by TLC. When the reaction was complete, the formed solid was washed with water (3 × 50 mL) and ethanol (2 × 20 mL) and the corresponding tryptanthrin was used in the next step without further purification.

8-Bromo-tryptanthrin (8-bromoindolo[2,1-b]quinazoline-6,12-dione) (1a)[104]. 5-Bromo-isatin (1.0 g, 1 equiv.), isatoic anhydride (0.866 g, 1.2 equiv.), K$_2$CO$_3$ (1.830 g, 3 equiv.) and DMF (20 mL) were used. The corresponding **1a** was obtained as a yellow solid (1.23 g, 85% yield).

2-Bromo-tryptanthrin (2-bromoindolo[2,1-b]quinazoline-6,12-dione) (1b)[104]. Isatin (0.75 g, 1 equiv.), 5-bromoisatoic anhydride (1.48 g, 1.2 equiv.), K$_2$CO$_3$ (2.11 g, 3 equiv.) and DMF (20 mL) were used. The corresponding **1b** was obtained as a yellow solid (1.59 g, 95% yield).

8-Bromo-2-fluoro-tryptanthrin (8-bromo-2-fluoroindolo[2,1-b]quinazoline-6,12-dione) (1c). 5-Bromoisatin (1.50 g, 1 equiv.), 5-fluoroisatoic anhydride (1.44 g, 1.2 equiv.), K$_2$CO$_3$ (2.75 g, 3 equiv.) and DMF (20 mL) were used. The corresponding **1c** was obtained as a yellow solid (1.69 g, 74% yield).

2-Bromo-8-fluoro-tryptanthrin (2-bromo-8-fluoroindolo[2,1-b]quinazoline-6,12-dione) (1d). 5-Fluoroisatin (1.0 g, 1 equiv.), 5-bromoisatoic anhydride (1.76 g, 1.2 equiv.), K$_2$CO$_3$ (2.75 g, 3 equiv.) and DMF (20 mL) were used. The corresponding **1d** was obtained as a yellow solid (1.70 g, 81% yield).

4.1.2. General procedure for the synthesis of boronate-tryptanthrin derivatives (2a–d). In a round-bottom flask or in a Radley's® 12-position carousel reactor tube under a nitrogen atmosphere were added the halide derivative (**1**), B$_2$NPG$_2$ (1.1 equiv.), PdCl$_2$(dppf) (3 mol%), KOAc (3 equiv.) and toluene. The reaction was stirred at 90 °C (in an oil bath when a round-bottom flask was used) overnight and monitored by TLC. The reaction was quenched with brine (30 mL) followed by extraction with CHCl$_3$ (3 × 30 mL). The combined organic phases were dried over MgSO$_4$, filtered and the solvent evaporated using a rotary evaporator. The crude mixture was filtered over a porous plate glass filter funnel packed with a layer of Celite and a layer of SiO$_2$ and eluted with CHCl$_3$ until the washings became colourless. After evaporation of the solvent the corresponding product (**2**) was obtained and used in the next steps.

8-(5,5-Dimethyl-1,3,2-dioxaborinan-2-yl)indolo[2,1-b]quinazoline-6,12-dione (2a). 8-Bromoindolo[2,1-b]quinazoline-6,12-dione (**1a**) (301.7 mg, 0.92 mmol), B$_2$NPG$_2$ (228 mg, 1.0 mmol, 1.1 equiv.), PdCl$_2$(dppf) (20.1 mg, 0.028 mmol, 3 mol%), KOAc (270 mg, 2.8 mmol, 3 equiv.) and toluene (4 mL) were used. The corresponding **2a** was obtained as a yellow-green solid (275.2 mg, 87% yield). M.p. = >220 °C. ^{1}H NMR (CDCl$_3$, 400 MHz): δ 1.04 (s, CH$_3$, 6H), 3.79 (s, CH$_2$, 4H), 7.63–7.67 (t, J = 8 Hz, Ar, 1H), 7.81–7.85 (t, J = 8 Hz, Ar, 1H), 8.00–8.02 (d, J = 8 Hz, Ar, 1H), 8.18–8.20 (d, J = 8 Hz, Ar, 1H), 8.34 (s, Ar, 1H), 8.41–8.43 (d, J = 8 Hz, Ar, 1H), 8.53–8.55 (d, J = 8 Hz, Ar, 1H). ^{13}C{^{1}H} APT NMR (CDCl$_3$, 100 MHz):

δ 22.00, 32.08, 72.57, 117.02, 121.42, 123.84, 127.67, 130.24, 130.80, 131.27, 135.21, 144.21, 146.78, 147.90, 158.25, 182.80. HRMS (ESI-TOF) *m/z*: calcd for $C_{20}H_{18}BN_2O_4$ $[M]^+$ 361.1760, found 361.0960.

2-(5,5-Dimethyl-1,3,2-dioxaborinan-2-yl)indolo[2,1-b]quinazoline-6,12-dione (2b). 2-Bromoindolo[2,1-*b*]quinazoline-6,12-dione (**1b**) (373 mg, 0.9 mmol), B₂NPG₂ (228 mg, 1.0 mmol, 1.1 equiv.), PdCl₂(dppf) (20.1 mg, 0.028 mmol, 3 mol%), KOAc (270 mg, 2.8 mmol, 3 equiv.) and toluene (4 mL) were used. The corresponding **2b** was obtained as a yellow solid (369.6 mg, >99% yield). M.p. = >220 °C. ¹H NMR (CDCl₃, 400 MHz): δ 1.05 (s, CH₃, 6H), 3.83 (s, CH₂, 4H), 7.39–7.43 (t, *J* = 8 Hz, Ar, 1H), 7.76–7.80 (t,*J* = 8 Hz, Ar, 1H), 7.90–7.91 (d,*J* = 8 Hz, Ar, 1H), 7.96–7.98 (d,*J* = 8 Hz, Ar, 1H), 8.22–8.24 (d,*J* = 8 Hz, Ar, 1H), 8.64–8.66 (d, *J* = 8 Hz, Ar, 1H), 8.88 (s, Ar, 1H). ¹³C{¹H} NMR (CDCl₃, 100 MHz): δ 22.03, 32.11, 72.62, 118.18, 122.05, 122.91, 125.48, 127.20, 129.76, 133.75, 138.39, 140.28, 144.80, 146.60, 148.24, 158.44, 182.87. HRMS (ESI-TOF) *m/z*: calcd for $C_{20}H_{18}BN_2O_4$ $[M]^+$ 361.1760, found 361.0957.

8-(5,5-Dimethyl-1,3,2-dioxaborinan-2-yl)-2-fluoroindolo[2,1-b]quinazoline-6,12-dione (2c). 8-Bromo-2-fluoroindolo[2,1-*b*]quinazoline-6,12-dione (**1c**) (332 mg, 0.8 mmol), B₂NPG₂ (216 mg, 0.9 mmol, 1.1 equiv.), PdCl₂(dppf) (19.1 mg, 0.026 mmol, 3 mol%), KOAc (256 mg, 2.6 mmol, 3 equiv.) and toluene (4 mL) were used. The corresponding **2c** was obtained as a yellow solid (292.8 mg, 80% yield). M.p. = >220 °C. ¹H NMR (CDCl₃, 400 MHz): δ 1.04 (s, CH₃, 6H), 3.80 (s, CH₂, 4H), 7.55–7.58 (m, Ar, 1H), 8.02–8.09 (m, Ar, 2H), 8.20–8.22 (d, *J* = 8 Hz, Ar, 1H), 8.36 (s, Ar, 1H), 8.54–8.56 (d, *J* = 8 Hz, Ar, 1H). ¹³C{¹H} NMR (CDCl₃, 100 MHz): δ 22.01, 32.11, 72.60, 113.27, 113.55, 117.08, 118.17, 121.50, 123.37, 123.61, 125.65, 127.61, 131.37, 133.26, 138.48, 143.43, 144.27, 147.66, 157.34, 182.31. HRMS (ESI-TOF) *m/z*: calcd for $C_{20}H_{17}BFN_2O_4$ $[M]^+$ 379.1740, found 379.0864.

2-(5,5-Dimethyl-1,3,2-dioxaborinan-2-yl)-8-fluoroindolo[2,1-b]quinazoline-6,12-dione (2d). 2-Bromo-8-fluoroindolo[2,1-*b*]quinazoline-6,12-dione (**1d**) (297 mg, 0.8 mmol), B2NPG2 (216 mg, 0.9 mmol, 1.1 equiv.), PdCl₂(dppf) (19.1 mg, 0.026 mmol, 3 mol%), KOAc (256 mg, 2.6 mmol, 3 equiv.) and toluene (4 mL) were used. The corresponding **2d** was obtained as a yellow solid (302 mg, 93% yield). M.p. = >220 °C. ¹H NMR (CDCl₃, 400 MHz): δ 1.05 (s, CH₃, 6H), 3.83 (s, CH₂, 4H), 7.46–7.50 (t, *J* = 8 Hz, Ar, 1H), 7.56–7.58 (d, *J* = 8 Hz, Ar, 1H), 7.96–7.98 (d,*J* = 8 Hz, Ar, 1H), 8.23–8.25 (d,*J* = 8 Hz, Ar, 1H), 8.65–8.66 (m, Ar, 1H), 8.87 (s, Ar, 1H). ¹³C{¹H} NMR (CDCl₃, 100 MHz): δ 22.03, 32.11, 72.62, 118.18, 122.05, 122.91, 124.31, 125.48, 127.20, 129.76, 132.72, 133.75, 138.39, 140.28, 144.80, 146.60, 148.24, 158.44, 182.87. MS (ESI) *m/z*: 333.09 (M − OHNa)⁺.

4.1.3. General procedure for the library generation *via* the Petasis 3-MCR. In a round-bottom flask or in a Radley's® 12-position carousel reactor tube was added the borylated tryptanthrin derivative (**2**) (0.3 mmol, 1.0 equiv.), the amine (3.9 equiv.), the aldehyde (3.3 equiv.), BINOL (20 mol%), MS 4 Å (200 mg) and CHCl₃ (3 mL). The reaction was stirred at 70 °C for 24 hours. After cooling down, the reaction mixture was filtered using a porous plate glass funnel packed with a Celite layer and washed with CHCl₃. The solvent was evaporated under reduced pressure and the crude product purified by silica gel flash chromatography using hexane/AcOEt from (5 : 1) to (1 : 1) as eluents.

8-((2-Hydroxyphenyl)(morpholino)methyl)indolo[2,1-b]quinazoline-6,12-dione (5aaa). **2a** (112 mg, 0.3 mmol, 1 equiv.), **3a** (0.1 mL, 1.1 mmol, 3.9 equiv.), **4a** (0.1 mL, 0.9 mmol, 3.3 equiv.), BINOL (15.9 mg, 0.06 mmol, 20 mol%), MS 4 Å (200 mg) and CHCl₃ (3 mL) were used to obtain the corresponding **5aaa** as a yellow solid (89.9 mg, 66% yield). M.p. = >220 °C. ¹H NMR (CDCl₃, 400 MHz): δ 2.48–2.51 (m, CH₂, 2H), 2.65 (s br, CH₂, 2H), 3.79 (s, CH₂, 4H), 4.50 (s, CH, 1H), 6.74–6.78 (t, *J* = 8 Hz, Ar, 1H), 6.88–6.90 (d, *J* = 8 Hz, Ar, 1H), 6.95–6.97 (d, *J* = 8 Hz, Ar, 1H), 7.14–7.18 (t, *J* = 8 Hz, Ar, 1H), 7.63–7.66 (t, Ar, 1H), 7.81–7.85 (t, *J* = 8 Hz, Ar, 1H), 7.87–7.89 (m, Ar, 1H), 7.96–8.00 (m, Ar, 2H), 8.38–8.40 (d, *J* = 8 Hz, Ar, 1H), 8.54–8.56 (d, *J* = 8 Hz, Ar, 1H), 11.29 (s br, OH, 1H). ¹³C{¹H} APT NMR (CDCl₃, 100 MHz): δ 52.47, 66.86, 76.15, 117.12, 118.66, 120.21, 122.53, 123.70, 125.30, 127.71, 129.22, 129.52, 130.52, 130.92, 135.35, 138.36, 139.26, 144.39, 145.98, 146.63, 155.91, 157.99, 182.23. HRMS (ESI-TOF) *m/z*: calcd for $C_{26}H_{22}O_4N_3$ $[M]^+$ 440.16048, found 440.1597.

8-((2-Hydroxyphenyl)(piperidin-1-yl)methyl)indolo[2,1-b]quinazoline-6,12-dione (5aca). **2a** (100 mg, 0.3 mmol, 1 equiv.), **3c** (0.1 mL, 1.1 mmol, 3.9 equiv.), **4a** (0.1 mL, 0.9 mmol, 3.3 equiv.), BINOL (15.9 mg, 0.06 mmol, 20 mol%), MS 4 Å (200 mg) and CHCl₃ (3 mL) were used to obtain the corresponding **5aca** as a green solid (32.1 mg, 26% yield). M.p. = 216.8 °C decomp. ¹H NMR (CDCl₃, 400 MHz): δ 1.49–1.67 (m, CH₂, 6H), 2.37–2.44 (m, CH₂, 4H), 4.55 (s, CH, 1H), 6.70–6.73 (t, Ar, 1H), 6.86–6.89 (m, Ar, 2H), 7.11–7.15 (t, *J* = 8 Hz, Ar, 1H), 7.61–7.64 (t, Ar, 1H), 7.79–7.84 (m, Ar, 2H), 7.92 (s, Ar, 1H), 7.97–7.99 (d, *J* = 8 Hz, Ar, 1H), 8.36–8.38 (d, *J* = 8 Hz, Ar, 1H), 8.51–8.53 (d, *J* = 8 Hz, Ar, 1H), 12.06 (s br, OH, 1H). ¹³C{¹H} NMR (CDCl₃, 100 MHz): δ 24.08, 26.08, 52.84, 75.85, 117.51, 118.44, 119.62, 122.33, 123.71, 124.44, 125.47, 127.66, 128.96, 129.10, 130.42, 130.86, 135.27, 138.57, 139.57, 144.48, 145.81, 146.65, 156.86, 157.96, 182.43. HRMS (ESI-TOF) *m/z*: calcd for $C_{27}H_{24}O_3N_3$ $[M]^+$ 438.18122, found 438.1803.

8-((3,4-Dihydroisoquinolin-2(1H)-yl)(2-hydroxyphenyl)methyl)indolo[2,1-b]quinazoline-6,12-dione (5ada). **2a** (122 mg, 0.3 mmol), **3d** (0.14 mL, 1.1 mmol, 3.9 equiv.), **4a** (0.1 mL, 0.9 mmol, 3.3 equiv.), BINOL (15.9 mg, 0.06 mmol, 20 mol%), MS 4 Å (200 mg) and CHCl₃ (3 mL) were used to obtain the corresponding **5ada** as a yellow solid (19.1 mg, 12% yield). M.p. = 215 °C decomp. ¹H NMR (CDCl₃, 400 MHz): δ 2.82–3.10 (m, CH₂, 4H), 3.71 (s, CH₂, 2H), 4.71 (s, CH, 1H), 6.76–6.80 (t, *J* = 8 Hz, Ar, 1H), 6.90–6.92 (m, Ar, 2H), 6.99–7.00 (m, Ar, 1H), 7.09–7.21 (m, Ar, 4H), 7.63–7.67 (t, *J* = 8 Hz, Ar, 2H), 7.81–7.85 (t,*J* = 8 Hz, Ar, 1H), 7.96–8.02 (m, Ar, 3H), 8.39–8.41 (d,*J* = 8 Hz, Ar, 1H), 8.56–8.58 (d, *J* = 8 Hz, Ar, 1H), 11.49 (s br, OH, 1H). ¹³C{¹H} NMR (CDCl₃, 100 MHz): δ 28.59, 49.23, 54.62, 75.16, 117.81, 118.70, 119.98, 122.51, 123.74, 124.34, 125.22, 126.27, 126.92, 127.02, 127.71, 128.78, 129.05, 129.38, 130.48, 130.92, 132.94,

133.44, 135.32, 138.24, 139.93, 144.47, 145.99, 146.67, 156.47, 158.01, 182.38. HRMS (ESI-TOF) *m/z*: calcd for $C_{31}H_{24}O_3N_3$ [M]$^+$ 486.18122, found 486.1805.

8-((3,5-Di-tert-butyl-2-hydroxyphenyl)(morpholino)methyl)indolo[2,1-b]quinazoline-6,12-dione (5aac). **2a** (88 mg, 0.3 mmol), **3a** (0.1 mL, 1.1 mmol, 3.9 equiv.), **4c** (215 mg, 0.9 mmol, 3.3 equiv.), BINOL (15.9 mg, 0.06 mmol, 20 mol%), MS 4 Å (200 mg) and CHCl$_3$ (3 mL) were used to obtain the corresponding **5aac** as a yellow solid (60.5 mg, 45% yield). M.p. = 217.2 °C decomp. ^{1}H NMR (CDCl$_3$, 400 MHz): δ 1.21 (s, CH$_3$, 9H), 1.44 (s, CH$_3$, 9H), 2.50–2.60 (m, CH$_2$, 4H), 3.79 (s, CH$_2$, 4H), 4.46 (s, CH, 1H), 6.80 (s, Ar, 1H), 7.20 (s, Ar, 1H), 7.63–7.67 (t, *J* = 8 Hz, Ar, 1H), 7.81–7.85 (t, *J* = 8 Hz, Ar, 1H), 7.95–8.02 (m, Ar, 3H), 8.40–8.42 (d, *J* = 8 Hz, Ar, 1H), 8.54–8.56 (d, *J* = 8 Hz, Ar, 1H), 11.45 (s br, OH, 1H). ^{13}C{^{1}H} NMR (CDCl$_3$, 100 MHz): δ 29.68, 31.72, 34.33, 35.23, 66.82, 77.05, 118.69, 122.45, 122.83, 123.76, 125.46, 127.74, 130.46, 130.93, 135.31, 137.08, 138.44, 139.79, 141.72, 144.51, 145.92, 146.71, 152.35, 158.03, 182.44. HRMS (ESI-TOF) *m/z*: calcd for $C_{34}H_{38}O_4N_3$ [M]$^+$ 552.2857, found 552.2850.

8-((5-Bromo-2-hydroxyphenyl)(morpholino)methyl)indolo[2,1-b]quinazoline-6,12-dione (5aad). **2a** (177 mg, 0.5 mmol), **3a** (0.17 mL, 1.9 mmol, 3.9 equiv.), **4d** (332 mg, 1.7 mmol, 3.3 equiv.), BINOL (28.6 mg, 0.1 mmol, 20 mol%), MS 4 Å (300 mg) and CHCl$_3$ (5 mL) were used to obtain the corresponding **5aad** as a green solid (147.4 mg, 58% yield). M.p. = 170 °C decomp. ^{1}H NMR (CDCl$_3$, 400 MHz): δ 2.29–2.62 (m, CH$_2$, 4H), 3.77 (s br, CH$_2$, 4H), 4.45 (s, CH, 1H), 6.77–6.79 (d, *J* = 8 Hz, Ar, 1H), 7.07 (s, Ar, 1H), 7.23–7.26 (m, Ar, 1H), 7.62–7.66 (t, *J* = 8 Hz, Ar, 1H), 7.82–7.84 (m, Ar, 2H), 7.93 (s, Ar, 1H), 7.97–7.99 (d, *J* = 8 Hz, Ar, 1H), 8.36–8.38 (d, *J* = 8 Hz, Ar, 1H), 8.55–8.57 (d, *J* = 8 Hz, Ar, 1H), 11.47 (s br, OH, 1H). ^{13}C{^{1}H} NMR (CDCl$_3$, 100 MHz): δ 66.77, 75.64, 111.78, 118.79, 119.66, 122.64, 123.68, 125.24, 125.73, 127.74, 130.58, 130.95, 131.73, 132.32, 135.41, 138.28, 138.45, 144.31, 146.16, 146.61, 155.18, 158.00, 182.23. HRMS (ESI-TOF) *m/z*: calcd for $C_{26}H_{21}O_4N_3Br$ [M]$^+$ 518.0710, found 518.0701.

8-((3-Ethoxy-2-hydroxyphenyl)(morpholino)methyl)indolo[2,1-b]quinazoline-6,12-dione (5aaf). **2a** (93 mg, 0.3 mmol), **3a** (0.1 mL, 1.1 mmol, 3.9 equiv.), **4f** (152 mg, 0.9 mmol, 3.3 equiv.), BINOL (15.9 mg, 0.06 mmol, 20 mol%), MS 4 Å (200 mg) and CHCl$_3$ (3 mL) were used to obtain the corresponding **5aaf** as a yellow solid (13.6 mg, 11% yield). M.p. = 137.5–138.2 °C. ^{1}H NMR (CDCl$_3$, 400 MHz): δ 1.47–1.50 (t, CH$_3$, 3H), 2.48–2.62 (m, CH$_2$, 4H), 3.77 (m, CH$_2$, 4H), 4.05–4.12 (q, CH$_2$, 2H), 4.58 (s, CH, 1H), 6.67–6.77 (m, Ar, 3H), 7.62–7.66 (t, *J* = 8 Hz, Ar, 1H), 7.80–7.84 (t, *J* = 8 Hz, Ar, 1H), 7.90–8.00 (m, Ar, 3H), 8.37–8.39 (d, *J* = 8 Hz, Ar, 2H), 8.51–8.53 (d, *J* = 8 Hz, Ar, 1H), 10.27 (s br, OH, 1H). ^{13}C{^{1}H} NMR (CDCl$_3$, 100 MHz): δ 15.01, 52.48, 64.40, 66.96, 73.93, 111.84, 118.54, 119.91, 120.47, 122.35, 123.70, 124.51, 125.31, 127.67, 130.45, 130.87, 135.30, 138.35, 139.97, 144.44, 145.05, 145.80, 146.61, 147.62, 157.95, 182.42. HRMS (ESI-TOF) *m/z*: calcd for $C_{28}H_{26}O_5N_3$ [M]$^+$ 484.1867, found 484.1858.

8-((2-Hydroxy-3-methoxyphenyl)(morpholino)methyl)indolo[2,1-b]quinazoline-6,12-dione (5aag). **2a** (121 mg, 0.3 mmol), **3a** (0.1 mL,

1.1 mmol, 3.9 equiv.), **4g** (140 mg, 0.9 mmol, 3.3 equiv.), BINOL (15.9 mg, 0.06 mmol, 20 mol%), MS 4 Å (200 mg) and CHCl$_3$ (3 mL) were used to obtain the corresponding **5aag** as a yellow solid (18.0 mg, 11% yield). M.p. = 165.2–167 °C. ^{1}H NMR (CDCl$_3$, 400 MHz): δ 2.49–2.64 (m, CH$_2$, 4H), 3.78 (s br, CH$_2$, 4H), 3.88 (s, OMe, 3H), 4.57 (s, CH, 1H), 6.66 (m, Ar, 1H), 6.74–6.78 (t, *J* = 8 Hz, Ar, 2H), 7.62–7.66 (t, *J* = 8 Hz, Ar, 1H), 7.80–7.84 (t, *J* = 8 Hz, Ar, 1H), 7.89–8.00 (m, Ar, 3H), 8.36–8.38 (d, *J* = 8 Hz, Ar, 1H), 8.51–8.53 (m, Ar, 1H), 10.75 (s br, OH, 1H). ^{13}C{^{1}H} NMR (CDCl$_3$, 100 MHz): δ 52.45, 56.00, 66.94, 74.51, 110.81, 118.61, 119.98, 120.63, 122.37, 123.68, 125.32, 127.68, 130.48, 130.88, 135.32, 138.36, 144.39, 145.00, 146.60, 157.95, 182.36. HRMS (ESI-TOF) *m/z*: calcd for $C_{27}H_{24}O_5N_3$ [M]$^+$ 470.1711, found 470.1702.

8-((3-(tert-Butyl)-2-hydroxyphenyl)(morpholino)methyl)indolo[2,1-b]quinazoline-6,12-dione (5aai). **2a** (102 mg, 0.3 mmol), **3a** (0.1 mL, 1.1 mmol, 3.9 equiv.), **4i** (163 mg, 0.9 mmol, 3.3 equiv.), BINOL (15.9 mg, 0.06 mmol, 20 mol%), MS 4 Å (200 mg) and CHCl$_3$ (3 mL) were used to obtain the corresponding **5aai** as a yellow solid (50 mg, 36% yield). M.p. = 254 °C decomp. ^{1}H NMR (CDCl$_3$, 400 MHz): δ 1.43 (s, CH$_3$, 9H), 2.45–2.70 (m, CH$_2$, 4H), 3.80 (s, CH$_2$, 4H), 4.49 (s, CH, 1H), 6.68–6.72 (t, *J* = 8 Hz, Ar, 1H), 6.82–6.84 (d, *J* = 8 Hz, Ar, 1H), 7.17–7.19 (d, *J* = 8 Hz, Ar, 1H), 7.65–7.69 (t, *J* = 8 Hz, Ar, 1H), 7.83–7.87 (t, *J* = 8 Hz, Ar, 1H), 7.92–8.03 (m, Ar, 3H), 8.41–8.43 (d, *J* = 8 Hz, Ar, 1H), 8.55–8.57 (d, *J* = 8 Hz, Ar, 1H), 11.73 (s, OH, 1H). ^{13}C{^{1}H} NMR (CDCl$_3$, 100 MHz): δ 29.40, 34.91, 66.68, 76.51, 118.54, 119.23, 123.54, 123.63, 125.25, 126.53, 127.08, 127.61, 130.35, 130.82, 135.20, 137.97, 138.16, 139.29, 145.82, 154.94, 163.24, 182.23. HRMS (ESI-TOF) *m/z*: calcd for $C_{30}H_{29}O_4N_3Na$ [M]$^+$ 518.2050, found 518.2042.

2-((2-Hydroxyphenyl)(morpholino)methyl)indolo[2,1-b]quinazoline-6,12-dione (5baa). **2b** (103 mg, 0.3 mmol), **3a** (0.1 mL, 1.1 mmol, 3.9 equiv.), **4a** (0.1 mL, 0.9 mmol, 3.3 equiv.), BINOL (15.9 mg, 0.06 mmol, 20 mol%), MS 4 Å (200 mg) and CHCl$_3$ (3 mL) were used to obtain the corresponding **5baa** as a yellow solid (100.9 mg, 80% yield). M.p. = 211.5 °C decomp. ^{1}H NMR (CDCl$_3$, 400 MHz): δ 2.45–2.65 (m, CH$_2$, 4H), 3.71–3.76 (m, CH$_2$, 4H), 4.60 (s, CH, 1H), 6.71–6.74 (t, Ar, 1H), 6.85–6.87 (d, *J* = 8 Hz, Ar, 1H), 6.97–6.99 (m, Ar, 1H), 7.10–7.14 (t, *J* = 8 Hz, Ar, 1H), 7.37–7.41 (t, *J* = 8 Hz, Ar, 1H), 7.73–7.77 (t, *J* = 8 Hz, Ar, 1H), 7.85–7.87 (d, *J* = 8 Hz, Ar, 1H), 7.93–7.95 (d, *J* = 8 Hz, Ar, 2H), 7.99 (m, Ar, 1H), 8.39 (s, Ar, 1H), 8.55–8.58 (d, *J* = 8 Hz, Ar, 1H), 11.37 (s br, OH, 1H). ^{13}C{^{1}H} NMR (CDCl$_3$, 100 MHz): δ 52.55, 66.86, 76.41, 117.64, 118.08, 120.20, 122.06, 123.71, 124.02, 125.62, 127.47, 127.51, 129.45, 129.53, 131.87, 134.87, 138.48, 142.37, 144.62, 146.31, 146.52, 155.94, 157.95, 182.46. HRMS (ESI-TOF) *m/z*: calcd for $C_{26}H_{22}O_4N_3$ [M]$^+$ 440.1605, found 440.1598.

2-((2-Hydroxyphenyl)(piperidin-1-yl)methyl)indolo[2,1-b]quinazoline-6,12-dione (5bca). **2b** (85 mg, 0.3 mmol), **3c** (0.1 mL, 1.1 mmol, 3.9 equiv.), **4a** (0.1 mL, 0.9 mmol, 3.3 equiv.), BINOL (15.9 mg, 0.06 mmol, 20 mol%), MS 4 Å (200 mg) and CHCl$_3$ (3 mL) were used to obtain the corresponding **5bca** as a green solid (61.8 mg, 60% yield). M.p. = 197.8 °C decomp. ^{1}H NMR (CDCl$_3$, 400 MHz): δ 1.48 (s br, CH$_2$, 2H), 1.65 (s br, CH$_2$, 4H), 2.42–2.62 (m, CH$_2$, 4H), 4.65 (s, CH, 1H), 6.68–6.71 (t, Ar, 1H), 6.85–6.87 (d, *J* = 8 Hz, Ar, 1H), 6.90–6.92 (d, *J* = 8 Hz, Ar, 1H),

7.09–7.13 (t, J = 8 Hz, Ar, 1H), 7.35–7.39 (t, J = 8 Hz, Ar, 1H), 7.70–7.74 (t, J = 8 Hz, Ar, 1H), 7.84–7.85 (d, J = 4 Hz, Ar, 1H), 7.92–7.97 (m, Ar, 2H), 8.36 (s, Ar, 1H), 8.54–8.56 (d, J = 8 Hz, Ar, 1H), 11.90 (s br, OH, 1H). ^{13}C{^{1}H} NMR (CDCl$_3$, 100 MHz): δ 24.06, 26.06, 76.10, 117.38, 117.93, 119.53, 121.97, 123.75, 124.51, 125.45, 127.34, 127.44, 129.01, 129.14, 131.50, 138.32, 142.80, 144.40, 146.21, 146.22, 156.83, 157.95, 182.40. HRMS (ESI-TOF) m/z: calcd for C$_{27}$H$_{24}$O$_4$N$_3$ [M]$^+$ 438.1812, found 438.1802.

2-((Benzyl)(methyl)amino)(2-hydroxyphenyl)methyl)indolo[2,1-b] quinazoline-6,12-dione (5bea). **2b** (107 mg, 0.3 mmol), **3e** (0.14 mL, 1.1 mmol, 3.9 equiv.), **4a** (0.1 mL, 0.9 mmol, 3.3 equiv.), BINOL (15.9 mg, 0.06 mmol, 20 mol%), MS 4 Å (200 mg) and CHCl$_3$ (3 mL) were used to obtain the corresponding **5bea** as a yellow solid (21.4 mg, 15% yield). M.p. = 194 °C decomp. ^{1}H NMR (CDCl$_3$, 400 MHz): δ 2.21 (s, CH$_3$, 3H), 3.56–3.79 (m, CH$_2$, 2H), 4.86 (s, CH, 1H), 6.74–6.78 (t, J = 8 Hz, Ar, 1H), 6.93–6.99 (m, Ar, 2H), 7.15–7.19 (t, J = 8 Hz, Ar, 1H), 7.27–7.37 (m, Ar, 5H), 7.39–7.43 (t, J = 8 Hz, Ar, 1H), 7.75–7.79 (t, J = 8 Hz, Ar, 1H), 7.88–7.90 (d, J = 8 Hz, Ar, 1H), 7.99–8.01 (m, Ar, 1H), 8.09–8.11 (m, Ar, 1H), 8.46 (s, Ar, 1H), 8.59–8.61 (d, J = 8 Hz, Ar, 1H), 11.95 (s br, OH, 1H). ^{13}C{^{1}H} NMR (CDCl$_3$, 100 MHz): δ 39.67, 60.01, 75.32, 117.60, 118.06, 119.83, 122.05, 123.94, 124.51, 125.58, 127.45, 127.63, 127.95, 128.85, 129.13, 129.40, 129.46, 131.69, 135.16, 138.52, 138.44, 142.49, 144.56, 146.31, 146.44, 156.63, 158.01, 182.48. HRMS (ESI-TOF) m/z: calcd for C$_{30}$H$_{24}$O$_3$N$_3$ [M]$^+$ 474.1812, found 474.1804.

2-((3,5-Di-tert-butyl-2-hydroxyphenyl)(morpholino)methyl)indolo [2,1-b]quinazoline-6,12-dione (5bac). **2b** (96 mg, 0.3 mmol), **3a** (0.1 mL, 1.1 mmol, 3.9 equiv.), **4c** (215 mg, 0.9 mmol, 3.3 equiv.), BINOL (15.9 mg, 0.06 mmol, 20 mol%), MS 4 Å (200 mg) and CHCl$_3$ (3 mL) were used to obtain the corresponding **5bac** as a yellow solid (20.3 mg, 14% yield). M.p. = 115.3–117 °C. ^{1}H NMR (CDCl$_3$, 400 MHz): δ 1.20 (s, CH$_3$, 9H), 1.45 (s, CH$_3$, 9H), 2.46–2.47 (m, CH$_2$, 4H), 3.74–3.78 (m, CH$_2$, 4H), 4.57 (s, CH, 1H), 6.83–6.84 (d, J = 8 Hz, Ar, 1H), 7.19–7.20 (d, J = 8 Hz, Ar, 1H), 7.38–7.41 (t, Ar, 1H), 7.72–7.77 (m, Ar, 1H), 7.87–7.88 (d, J = 4 Hz, Ar, 1H), 7.93–7.95 (d, J = 8 Hz, Ar, 1H), 8.05–8.09 (m, Ar, 1H), 8.46 (s br, Ar, 1H), 8.57–8.59 (d, J = 8 Hz, Ar, 1H), 11.60 (s br, OH, 1H). ^{13}C{^{1}H} NMR (CDCl$_3$, 100 MHz): δ 29.67, 31.70, 34.29, 35.22, 66.83, 77.30, 118.04, 122.01, 122.81, 123.70, 123.91, 124.00, 125.55, 127.41, 127.59, 129.60, 131.74, 135.11, 136.95, 138.42, 141.55, 142.95, 144.48, 146.28, 146.31, 152.42, 158.01, 182.52. HRMS (ESI-TOF) m/z: calcd for C$_{34}$H$_{38}$O$_4$N$_3$ [M]$^+$ 552.2857, found 552.2844.

2-((5-Bromo-2-hydroxyphenyl)(morpholino)methyl)indolo[2,1-b] quinazoline-6,12-dione (5bad). **2b** (95 mg, 0.3 mmol), **3a** (0.1 mL, 1.1 mmol, 3.9 equiv.), **4d** (184 mg, 0.9 mmol, 3.3 equiv.), BINOL (15.9 mg, 0.06 mmol, 20 mol%), MS 4 Å (200 mg) and CHCl$_3$ (3 mL) were used to obtain the corresponding **5bad** as a green solid (80.3 mg, 59% yield). M.p. = 179.1–183 °C. ^{1}H NMR (CDCl$_3$, 400 MHz): δ 2.45–2.64 (m, CH$_2$, 4H), 3.77 (m, CH$_2$, 4H), 4.55 (s, CH, 1H), 6.77–6.79 (d, J = 8 Hz, Ar, 1H), 7.09–7.10 (d, J = 4 Hz, Ar, 1H), 7.22–7.24 (d, J = 8 Hz, Ar, 1H), 7.40–7.44 (t, J = 8 Hz, Ar, 1H), 7.76–7.80 (t, J = 8 Hz, Ar, 1H), 7.88–7.90

(d, J = 8 Hz, Ar, 1H), 7.97–7.99 (m, Ar, 2H), 8.39 (s, Ar, 1H), 8.58–8.60 (d, J = 8 Hz, Ar, 1H), 11.56 (s br, OH, 1H). ^{13}C{^{1}H} NMR (CDCl$_3$, 100 MHz): δ 66.78, 75.91, 117.71, 118.06, 119.57, 121.99, 124.11, 125.63, 125.76, 127.45, 127.55, 131.89, 131.95, 132.27, 134.73, 138.52, 141.55, 144.71, 146.24, 146.68, 155.19, 157.83, 182.40. HRMS (ESI-TOF) m/z: calcd for C$_{26}$H$_{21}$O$_4$N$_3$Br [M]$^+$ 518.0710, found 518.0701.

2-((3-Ethoxy-2-hydroxyphenyl)(morpholino)methyl)indolo[2,1-b] quinazoline-6,12-dione (5baf). **2b** (99 mg, 0.3 mmol), **3a** (0.1 mL, 1.1 mmol, 3.9 equiv.), **4f** (152 mg, 0.9 mmol, 3.3 equiv.), BINOL (15.9 mg, 0.06 mmol, 20 mol%), MS 4 Å (200 mg) and CHCl$_3$ (3 mL) were used to obtain the corresponding **5baf** as a yellow solid (47.7 mg, 36% yield). M.p. = 99.8–101.2 °C. ^{1}H NMR (CDCl$_3$, 400 MHz): δ 1.44–1.48 (t, J = 8 Hz, CH$_3$, 3H), 2.44–2.63 (m, CH$_2$, 4H), 3.71–3.80 (m, CH$_2$, 4H), 4.02–4.07 (q, CH$_2$, 2H), 4.67 (s, CH, 1H), 6.68–6.75 (m, Ar, 3H), 7.34–7.38 (t, J = 8 Hz, Ar, 1H), 7.70–7.74 (t, J = 8 Hz, Ar, 1H), 7.82–7.84 (d, J = 8 Hz, Ar, 1H), 7.90–7.92 (d, J = 8 Hz, Ar, 1H), 8.02–8.06 (m, Ar, 1H), 8.38 (s, Ar, 1H), 8.52–8.54 (d, J = 8 Hz, Ar, 1H), 10.61 (s br, OH, 1H). ^{13}C{^{1}H} NMR (CDCl$_3$, 100 MHz): δ 14.95, 52.45, 64.29, 66.87, 74.51, 111.87, 117.90, 119.77, 120.71, 121.92, 123.73, 124.39, 125.44, 127.30, 127.33, 131.63, 134.75, 138.31, 142.93, 144.36, 145.09, 146.15, 146.20, 147.60, 157.86, 182.36. HRMS (ESI-TOF) m/z: calcd for C$_{28}$H$_{26}$O$_5$N$_3$ [M]$^+$ 484.1867, found 484.1859.

2-((2-Hydroxy-3-methoxyphenyl)(morpholino)methyl)indolo[2,1-b] quinazoline-6,12-dione (5bag). **2b** (94 mg, 0.3 mmol), **3a** (0.1 mL, 1.1 mmol, 3.9 equiv.), **4g** (140 mg, 0.9 mmol, 3.3 equiv.), BINOL (15.9 mg, 0.06 mmol, 20 mol%), MS 4 Å (200 mg) and CHCl$_3$ (3 mL) were used to obtain the corresponding **5bag** as a yellow solid (22.3 mg, 18% yield). M.p. = 133.8–135 °C. ^{1}H NMR (CDCl$_3$, 400 MHz): δ 2.46–2.66 (m, CH$_2$, 4H), 3.77–3.81 (m, CH$_2$, 4H), 3.87 (s, OMe, 3H), 4.67 (s, CH, 1H), 6.66–6.77 (m, Ar, 3H), 7.38–7.42 (t, J = 8 Hz, Ar, 1H), 7.74–7.78 (t, J = 8 Hz, Ar, 1H), 7.86 (m, Ar, 1H), 7.93–7.95 (d, J = 8 Hz, Ar, 1H), 8.03–8.08 (m, Ar, 1H), 8.39–8.40 (m, Ar, 1H), 8.57–8.59 (d, J = 8 Hz, Ar, 1H), 11.04 (s br, OH, 1H). ^{13}C{^{1}H} NMR (CDCl$_3$, 100 MHz): δ 52.50, 55.96, 66.92, 75.11, 110.83, 118.00, 119.90, 120.90, 121.99, 123.84, 124.24, 125.55, 127.41, 127.43, 129.57, 134.79, 138.42, 142.68, 144.48, 145.07, 146.24, 146.36, 148.42, 157.93, 182.44. HRMS (ESI-TOF) m/z: calcd for C$_{27}$H$_{24}$O$_5$N$_3$ [M]$^+$ 470.1711, found 470.1702.

2-Fluoro-8-((2-hydroxyphenyl)(morpholino)methyl)indolo[2,1-b] quinazoline-6,12-dione (5caa). **2c** (108 mg, 0.26 mmol), **3a** (0.1 mL, 1.1 mmol, 3.9 equiv.), **4a** (0.1 mL, 0.9 mmol, 3.3 equiv.), BINOL (14.9 mg, 0.05 mmol, 20 mol%), MS 4 Å (200 mg) and CHCl$_3$ (3 mL) were used to obtain the corresponding **5caa** as a yellow solid (12.7 mg, 10% yield). M.p. = 210.3 °C decomp. ^{1}H NMR (CDCl$_3$, 400 MHz): δ 2.48–2.51 (m, CH$_2$, 2H), 2.65 (m, CH$_2$, 2H), 3.79 (m, CH$_2$, 4H), 4.51 (s, CH, 1H), 6.75–6.78 (t, Ar, 1H), 6.88–6.90 (d, J = 8 Hz, Ar, 1H), 6.96–6.98 (d, J = 8 Hz, Ar, 1H), 7.14–7.18 (t, J = 8 Hz, Ar, 1H), 7.52–7.57 (m, Ar, 1H), 7.89–7.91 (d, J = 8 Hz, Ar, 1H), 7.97–8.05 (m, Ar, 3H), 8.53–8.55 (d, J = 8 Hz, Ar, 1H), 11.29 (s br, OH, 1H). ^{13}C{^{1}H} NMR (CDCl$_3$, 100 MHz): δ 52.50, 66.84, 76.13, 113.36, 113.60, 117.75, 118.73, 120.26, 122.63, 123.48, 123.64, 123.72, 125.39, 125.56, 125.65, 129.11,

129.58, 133.31, 133.40, 138.39, 139.54, 143.25, 143.93, 145.73, 155.89, 157.13, 162.07, 164.60, 182.00. HRMS (ESI-TOF) *m/z*: calcd for $C_{26}H_{21}O_4N_3F$ [M]$^+$ 458.1511, found 458.1503.

8-((3-(tert-Butyl)-2-hydroxyphenyl)(morpholino)methyl)-2-fluoroindolo[2,1-b]quinazoline-6,12-dione (5cai). **2c** (100 mg, 0.26 mmol), **3a** (0.1 mL, 1.1 mmol, 3.9 equiv.), **4i** (155 mg, 0.9 mmol, 3.3 equiv.), BINOL (14.9 mg, 0.05 mmol, 20 mol%), MS 4 Å (200 mg) and CHCl$_3$ (3 mL) were used to obtain the corresponding **5cai** as a yellow solid (21 mg, 16% yield). M.p. = 253 °C decomp. ^{1}H NMR (CDCl$_3$, 400 MHz): δ 1.43 (s, CH$_3$, 9H), 2.51–2.66 (m, CH$_2$, 4H), 3.80 (s, CH$_2$, 4H), 4.49 (s, CH, 1H), 6.68–6.72 (t,J = 8 Hz, Ar, 1H), 6.81–6.83 (d, J = 8 Hz, Ar, 1H), 7.17–7.19 (d,J = 8 Hz, Ar, 1H), 7.53–7.57 (t,J = 8 Hz, Ar, 1H), 7.93–8.07 (m, Ar, 4H), 8.54–8.56 (d,J = 8 Hz, Ar, 1H), 11.71 (s, OH, 1H). ^{13}C{^{1}H} NMR (CDCl$_3$, 100 MHz): δ 29.39, 34.91, 66.67, 76.51, 113.23, 113.48, 118.58, 119.25, 123.32, 123.50, 123.56, 125.32, 126.56, 127.07, 133.18, 133.27, 138.01, 138.18, 139.61, 143.19, 143.81, 143.84, 145.54, 154.93, 181.90. HRMS (ESI-TOF) *m/z*: calcd for $C_{30}H_{27}O_4N_3F$ [M]$^-$ 512.1991, found 512.1990.

8-Fluoro-2-((2-hydroxyphenyl)(morpholino)methyl)indolo[2,1-b]quinazoline-6,12-dione (5daa). **2d** (90 mg, 0.26 mmol), **3a** (0.1 mL, 1.1 mmol, 3.9 equiv.), **4a** (0.1 mL, 0.9 mmol, 3.3 equiv.), BINOL (14.9 mg, 0.05 mmol, 20 mol%), MS 4 Å (200 mg) and CHCl$_3$ (3 mL) were used to obtain the corresponding **5daa** as a yellow solid (22.1 mg, 20% yield). M.p. = 193.5 °C decomp. ^{1}H NMR (CDCl$_3$, 400 MHz): δ 2.52–2.69 (m, CH$_2$, 4H), 3.80 (m, CH$_2$, 4H), 4.68 (s, CH, 1H), 6.74–6.78 (t,J = 8 Hz, Ar, 1H), 6.88–6.90 (d,J = 8 Hz, Ar, 1H), 7.05 (s, Ar, 1H), 7.13–7.17 (t,J = 8 Hz, Ar, 1H), 7.44–7.49 (m, Ar, 1H), 7.53–7.56 (m, Ar, 1H), 7.94–7.96 (d,J = 8 Hz, Ar, 1H), 8.07 (s, Ar, 1H), 8.41 (s, Ar, 1H), 8.57–8.60 (m, Ar, 1H), 11.45 (s br, OH, 1H). ^{13}C{^{1}H} NMR (CDCl$_3$, 100 MHz): δ 52.52, 66.64, 112.15, 112.40, 117.59, 119.71, 119.79, 120.28, 123.41, 123.49, 123.94, 124.89, 125.12, 127.46, 129.40, 129.61, 131.96, 134.98, 142.39, 144.56, 146.34, 155.82, 157.66, 160.04, 162.54, 181.54. HRMS (ESI-TOF) *m/z*: calcd for $C_{26}H_{21}O_4N_3F$ [M]$^+$ 458.1511, found 458.1501.

8-Fluoro-2-((2-hydroxyphenyl)(piperidin-1-yl)methyl)indolo[2,1-b]quinazoline-6,12-dione (5dca). **2d** (77 mg, 0.26 mmol), **3c** (0.1 mL, 1.1 mmol, 3.9 equiv.), **4a** (0.1 mL, 0.9 mmol, 3.3 equiv.), BINOL (14.9 mg, 0.05 mmol, 20 mol%), MS 4 Å (200 mg) and CHCl$_3$ (3 mL) were used to obtain the corresponding **5dca** as a yellow solid (32 mg, 34% yield). M.p. = 209.9 °C decomp. ^{1}H NMR (CDCl$_3$, 400 MHz): δ 1.49–1.67 (m, CH$_2$, 6H), 2.45 (m, CH$_2$, 4H), 4.69 (s, CH, 1H), 6.69–6.73 (t, J = 8 Hz, Ar, 1H), 6.86–6.88 (d,J = 8 Hz, Ar, 1H), 6.95 (s, Ar, 1H), 7.10–7.14 (t,J = 8 Hz, Ar, 1H), 7.43–7.48 (m, Ar, 1H), 7.53–7.55 (m, Ar, 1H), 7.93–7.95 (d,J = 8 Hz, Ar, 1H), 8.02 (s, Ar, 1H), 8.37 (s, Ar, 1H), 8.57–8.61 (m, Ar, 1H), 12.13 (s br, OH, 1H). ^{13}C{^{1}H} NMR (CDCl$_3$, 100 MHz): δ 24.02, 25.94, 52.97, 75.89, 112.09, 112.34, 117.44, 119.70, 119.77, 113.43, 123.51, 123.78, 124.35, 124.83, 125.07, 127.47, 129.16, 131.73, 135.22, 142.41, 142.43, 143.06, 144.41, 146.16, 156.74, 157.78, 160.00, 162.49, 181.58. HRMS (ESI-TOF) *m/z*: calcd for $C_{27}H_{23}O_3N_3F$ [M]$^+$ 456.1718, found 456.1709.

2-((5-Bromo-2-hydroxyphenyl)(morpholino)methyl)-8-fluoroindolo[2,1-b]quinazoline-6,12-dione (5dad). **2d** (75 mg, 0.26 mmol), **3a** (0.1 mL, 1.1 mmol, 3.9 equiv.), **4d** (172.5 mg, 0.9 mmol, 3.3 equiv.), BINOL (14.9 mg, 0.05 mmol, 20 mol%), MS 4 Å (200 mg) and CHCl$_3$ (3 mL) were used to obtain the corresponding **5dad** as a yellow solid (16.5 mg, 16% yield). M.p. = 192.2–194 °C. ^{1}H NMR (CDCl$_3$, 400 MHz): δ 2.54–2.69 (m, CH$_2$, 4H), 3.81 (s, CH$_2$, 4H), 4.62 (s, CH, 1H), 6.81–6.83 (d,J = 8 Hz, Ar, 1H), 7.17 (s br, Ar, 1H), 7.24 (s, Ar, 1H), 7.48–7.52 (m, Ar, 1H), 7.56–7.58 (m, Ar, 1H), 7.97–8.03 (m, Ar, 2H), 8.42 (s, Ar, 1H), 8.59–8.62 (m, Ar, 1H), 11.62 (s br, OH, 1H). ^{13}C{^{1}H} NMR (CDCl$_3$, 100 MHz): δ 52.53, 66.58, 75.71, 111.87, 112.26, 112.50, 119.60, 119.79, 119.87, 123.41, 123.49, 124.13, 125.01, 125.25, 127.51, 131.92, 132.15, 132.47, 142.39, 144.71, 146.61, 155.11, 157.61, 160.12, 162.61, 181.57. HRMS (ESI-TOF) *m/z*: calcd for $C_{26}H_{20}O_4N_3BrF$ [M]$^+$ 536.0616, found 536.0609.

4.2. Antimicrobial activity evaluation

The antifungal activity was evaluated against nine fungal strains: two yeasts (*Candida albicans* ATCC 10231 and *Candida krusei* ATCC 6258); three filamentous fungi (*Aspergillus fumigatus* ATCC 204305, *Aspergillus niger* ATCC 16404 and *Mucor* spp.); and four clinical dermatophyte strains (*Trichophyton rubrum* FF5, *Trichophyton mentagrophytes* FF7, *Microsporum canis* FF1, and *Nannizzia gypsea* FF3 (formerly *Microsporum gypseum*)). The antibacterial activity was evaluated against Gram-negative bacteria (*Escherichia coli* ATCC 25922) and Gram-positive bacteria (*Staphylococcus aureus* ATCC 25923).

4.2.1. Antimicrobial susceptibility testing. MICs and MLCs were used for defining the antimicrobial activity in agreement with the references of the Clinical and Laboratory Standards Institute (CLSI) for broth microdilution tests, with minor modifications:[100] M27-A3 for yeasts, M38-A2 for filamentous fungi and dermatophytes and M100-A25 for bacteria.

A stock solution of the tryptanthrin derivatives was prepared in dimethyl sulfoxide (DMSO, Sigma-Aldrich, St. Louis, MO, USA). Two-fold serial dilutions in RPMI for fungi and in MHB2 for bacteria were prepared (concentration range 32–512 µg mL^{-1}) and distributed in sterile and disposable 96-flat-bottom-well microtiter plates. The final concentration of DMSO, used in growth control, did not interfere with the bacterial/fungal growth. Furthermore, two other controls were performed: a sterility control and a quality control, performed using an ATCC reference strain, bacteria with gentamicin (Sigma-Aldrich, Seelze, Germany) and yeast with voriconazole (kindly provided by Pfizer). Equal volumes of cell suspension and sample dilutions were added in the wells.

MICs were determined as the lowest concentrations resulting in 100% growth inhibition, in comparison with the sample-free controls. From wells showing no visible growth, 10 µL of culture were collected and deposited on MHA plates (for bacteria) and SDA (for fungi) to evaluate the MLC, defined as the lowest concentration at which no colonies grew after an incubation of 16–18 h/35 °C for bacteria, 48 h/35 °C for yeasts, *Aspergillus* and *Mucor*, and 5 days/25 °C for dermatophytes.

The library of 20 tryptanthrin derivatives, and the enantiomerically pure version of **5aaa** were tested at least two times against bacterial and fungal strains.

4.2.1.1. Antibacterial susceptibility testing. Pure cultures on MHA/24 h were used to obtain cell suspensions in sterile saline at a MacFarland standard of 0.5 (530 nm), corresponding to $1–5 \times 10^6$ cells per mL. The suspension was then diluted in MHB2 to get an inoculum suspension of $1–5 \times 10^4$ CFU per mL. The plates were incubated aerobically/35 °C/24 h. Gentamicine ($0.06–4$ µg mL^{-1}) and *E. coli* (ATCC 25922) were used as quality controls, results being within the recommended limits defined by CLSI.

4.2.1.2. Antifungal susceptibility testing. Yeast cell suspensions were prepared from pure cultures on SDA/24 h, in sterile saline solution and adjusted to the MacFarland standard of 0.5 at 530 nm, corresponding to an initial suspension of $1–5 \times 10^6$ CFU per mL. This suspension was diluted in RPMI to obtain an inoculum of $1–5 \times 10^3$ CFU per mL. For filamentous fungi, a spore suspension was prepared from pure culture with spores in SDA (*Aspergillus* and *Mucor*) or MYC (dermatophytes) in sterile saline with one drop of TW20 added. The spore density was evaluated by the spore count and diluted in RPMI to obtain $1–3 \times 10^3$ CFU per mL for dermatophytes and $0.4–5 \times 10^4$ CFU per mL for *Aspergillus* and *Mucor*. The plates were incubated aerobically at 35 °C/48 h for *C. albicans*, *Aspergillus* and *Mucor*, and at 25 °C/5–7 days for the dermatophytes. Voriconazole ($0.06–2$ µg mL^{-1}) and *C. krusei* ATCC 6258 were used as quality controls, with the results being within the recommended limits defined by CLSI.

Conflicts of interest

There are no conflicts to declare.

Acknowledgements

References

1 S. L. Schreiber, *Science*, 2000, **287**, 1964–1969.
2 W. R. J. D. Galloway, A. Isidro-Llobet and D. R. Spring, *Nat. Commun.*, 2010, **1**, 80.
3 S. Dandapani and L. A. Marcaurelle, *Curr. Opin. Chem. Biol.*, 2010, **14**, 362–370.
4 J. E. Biggs-Houck, A. Younai and J. T. Shaw, *Curr. Opin. Chem. Biol.*, 2010, **14**, 371–382.
5 R. C. Cioc, E. Ruijter and R. V. A. Orru, *Green Chem.*, 2014, **16**, 2958–2975.
6 P. Slobbe, E. Ruijter and R. V. A. Orru, *MedChemComm*, 2012, **3**, 1189–1218.
7 J. Kim, H. Kim and S. B. Park, *J. Am. Chem. Soc.*, 2014, **136**, 14629–14638.
8 C. S. Graebin, F. V. Ribeiro, K. R. Rogério and A. E. Kümmerle, *Curr. Org. Synth.*, 2019, **16**, 855–899.
9 D. Insuasty, J. Castillo, D. Becerra, H. Rojas and R. Abonia, *Molecules*, 2020, **25**, 505.
10 P. Brandão, C. Marques, A. J. Burke and M. Pineiro, *Eur. J. Med. Chem.*, 2021, **211**, 113102.
11 P. Brandão, C. S. Marques, E. P. Carreiro, M. Pineiro and A. J. Burke, *Chem. Rec.*, 2021, **21**, 924.
12 N. A. Petasis and I. Akritopoulou, *Tetrahedron Lett.*, 1993, **34**, 583–586.
13 N. R. Candeias, F. Montalbano, P. M. S. D. Cal and P. M. P. Gois, *Chem. Rev.*, 2010, **110**, 6169–6193.
14 P. Wu and T. E. Nielsen, *Drug Discovery Today: Technol.*, 2018, **29**, 27–33.
15 P. Wu, M. Givskov and T. E. Nielsen, *Chem. Rev.*, 2019, **119**, 11245–11290.
16 C. S. Marques, P. McArdle, A. Erxleben and A. J. Burke, *Eur. J. Org. Chem.*, 2020, 3622–3634.
17 P. Brandão, D. Pinheiro, J. S. S. de Melo and M. Pineiro, *Dyes Pigm.*, 2020, **173**, 107935.
18 A. M. Tucker and P. Grundt, *ARKIVOC*, 2012, 546–569, DOI: 10.3998/ark.5550190.0013.113,.
19 Y. Jahng, *Arch. Pharmacal Res.*, 2013, **36**, 517–535.
20 R. Kaur, S. K. Manjal, R. K. Rawal and K. Kumar, *Bioorg. Med. Chem.*, 2017, **25**, 4533–4552.
21 J. Hesse-Macabata, B. Morgner, P. Elsner, U. C. Hipler and C. Wiegand, *Sci. Rep.*, 2020, **10**, 1863.
22 D. C. M. Costa, M. M. B. de Azevedo, D. O. E. Silva, M. T. V. Romanos, T. Souto-Padron, C. S. Alviano and D. S. Alviano, *Nat. Prod. Res.*, 2017, **31**, 2077–2080.
23 J. S. Mani, J. B. Johnson, J. C. Steel, D. A. Broszczak, P. M. Neilsen, K. B. Walsh and M. Naiker, *Virus Res.*, 2020, **284**, 197989.
24 L. J. Xu, W. Jiang, H. Jia, L. S. Zheng, J. G. Xing, A. L. Liu and G. H. Du, *Front. Cell. Infect. Microbiol.*, 2020, **10**, 16.
25 Y. C. Tsai, C. L. Lee, H. R. Yen, Y. S. Chang, Y. P. Lin, S. H. Huang and C. W. Lin, *Biomolecules*, 2020, **10**, 366.
26 C. Pergola, B. Jazzar, A. Rossi, H. Northoff, M. Hamburger, L. Sautebin and O. Werz, *Br. J. Pharmacol.*, 2012, **165**, 765–776.
27 N. R. Han, P. D. Moon, H. M. Kim and H. J. Jeong, *Arch. Biochem. Biophys.*, 2014, **542**, 14–20.
28 I. G. Agafonova and T. V. Moskovkina, *Appl. Magn. Reson.*, 2015, **46**, 781–791.
29 Y. W. Kwon, S. Y. Cheon, S. Y. Park, J. Song and J. H. Lee, *Front. Cell. Neurosci.*, 2017, **11**, 18.

30 S. Lee, D. C. Kim, H. Y. Baek, K. D. Lee, Y. C. Kim and H. Oh, *Arch. Pharmacal Res.*, 2018, **41**, 419–430.

31 Z. Wang, X. Wu, C. L. Wang, L. Wang, C. Sun, D. B. Zhang, J. L. Liu, Y. N. Liang, D. X. Tang and Z. S. Tang, *Molecules*, 2018, **23**, 1062.

32 S. Kawaguchi, H. Sakuraba, H. Kikuchi, N. Numao, T. Asari, H. Hiraga, J. L. Ding, T. Matsumiya, K. Seya, S. Fukuda and T. Imaizumi, *Mol. Immunol.*, 2021, **129**, 32–38.

33 E. H. Jung, J. Y. Jung, H. L. Ko, J. K. Kim, S. M. Park, D. H. Jung, C. A. Park, Y. W. Kim, S. K. Ku, I. J. Cho and S. C. Kim, *Arch. Pharmacal Res.*, 2017, **40**, 1071–1086.

34 K. Iwaki, E. Ohashi, N. Arai, K. Kohno, S. Ushio, M. Taniguchi and S. Fukuda, *J. Ethnopharmacol.*, 2011, **134**, 450–459.

35 N. R. Han, H. M. Kim and H. J. Jeong, *Biomed. Pharmacother.*, 2016, **79**, 71–77.

36 S. Miao, X. P. Shi, H. Zhang, S. W. Wang, J. Y. Sun, W. Hua, Q. Miao, Y. Zhao and C. Q. Zhang, *Int. J. Mol. Sci.*, 2011, **12**, 3831–3845.

37 X. M. Liao, X. L. Zhou, N. K. Mak and K. N. Leung, *PLoS One*, 2013, **8**, e82294.

38 G. M. Shankar, V. V. Alex, A. A. Nisthul, S. V. Bava, S. Sundaram, A. P. Retnakumari, S. Chittalakkottu and R. J. Anto, *Cell Proliferation*, 2020, **53**, e12710.

39 Q. F. Zeno, C. R. Luo, J. L. Cho, D. N. Lai, X. C. Shen, X. Y. Zhang and W. Zhou, *Acta Pharm.*, 2021, **71**, 245–266.

40 H. N. Chang, Y. C. Yeh, H. Y. Chueh and J. H. S. Pang, *Phytomedicine*, 2019, **58**, 152879.

41 X. M. Liao and K. N. Leung, *Chem.-Biol. Interact.*, 2013, **203**, 512–521.

42 H. M. Cheng, Y. Z. Kuo, C. Y. Chang, C. H. Chang, W. Y. Fang, C. N. Chang, S. C. Pan, J. Y. Lin and L. W. Wu, *J. Ethnopharmacol.*, 2020, **255**, 112760.

43 L. N. Kirpotina, I. A. Schepetkin, D. Hammaker, A. Kuhs, A. I. Khlebnikov and M. T. Quinn, *Front. Pharmacol.*, 2020, **11**, 1145.

44 E. A. Jahne, D. E. Eigenmann, C. Sampath, V. Butterweck, M. Culot, R. Cecchelli, F. Gosselet, F. R. Walter, M. A. Deli, M. Smiesko, M. Hamburger and M. Oufir, *Planta Med.*, 2016, **82**, 1021–1029.

45 X. Y. Zhang, J. Xia, W. J. Zhang, Y. Luo, W. B. Sun and W. Zhou, *Integr. Med. Res.*, 2017, **6**, 269–279.

46 J. L. Liang, S. E. Park, Y. Kwon and Y. Jahng, *Bioorg. Med. Chem.*, 2012, **20**, 4962–4967.

47 S. S. Yang, X. S. Li, F. F. Hu, Y. L. Li, Y. Y. Yang, J. K. Yan, C. X. Kuang and Q. Yang, *J. Med. Chem.*, 2013, **56**, 8321–8331.

48 A. S. Pathania, S. Kumar, S. K. Guru, S. Bhushan, P. R. Sharma, S. K. Aithagani, P. P. Singh, R. A. Vishwakarma, A. Kumar and F. Malik, *PLoS One*, 2014, **9**, e110411.

49 K. Y. Jun, S. E. Park, J. L. Liang, Y. Jahng and Y. Kwon, *ChemMedChem*, 2015, **10**, 827–835.

50 S. N. Zhang, F. F. Qi, X. Fang, D. Yang, H. R. Hu, Q. Huang, C. X. Kuang and Q. Yang, *Eur. J. Med. Chem.*, 2018, **160**, 133–145.

51 D. Yang, S. N. Zhang, X. Fang, L. L. Guo, N. Hu, Z. L. Guo, X. S. Li, S. S. Yang, J. C. He, C. X. Kuang and Q. Yang, *J. Med. Chem.*, 2019, **62**, 9161–9174.

52 X. D. Zheng, B. L. Hou, R. Wang, Y. Y. Wang, C. L. Wang, H. Chen, L. Liu, J. L. Wang, X. M. Ma and J. L. Liu, *Tetrahedron*, 2019, **75**, 130351.

53 E. Catanzaro, N. Betari, J. M. Arencibia, S. Montanari, C. Sissi, A. De Simone, I. Vassura, A. Santini, V. Andrisano, V. Tumiatti, M. De Vivo, D. V. Krysko, M. B. Rocchi, C. Fimognari and A. Milelli, *Eur. J. Med. Chem.*, 2020, **202**, 112504.

54 Y. Y. Li, S. N. Zhang, R. Wang, M. H. Cui, W. Liu, Q. Yang and C. X. Kuang, *Bioorg. Med. Chem. Lett.*, 2020, **30**, 127159.

55 A. Popov, A. Klimovich, O. Styshova, T. Moskovkina, A. Shchekotikhin, N. Grammatikova, L. Dezhenkova, D. Kaluzhny, P. Deriabin, A. Gerasimenko, A. Udovenko and V. Stonik, *Int. J. Mol. Med.*, 2020, **46**, 1335–1346.

56 I. A. Schepetkin, A. I. Khlebnikov, A. S. Potapov, A. R. Kovrizhina, V. V. Matveevskaya, M. L. Belyanin, D. N. Atochin, S. O. Zanoza, N. M. Gaidarzhy, S. A. Lyakhov, L. N. Kirpotina and M. T. Quinn, *Eur. J. Med. Chem.*, 2019, **161**, 179–191.

57 J. M. Hwang, T. Oh, T. Kaneko, A. M. Upton, S. G. Franzblau, Z. K. Ma, S. N. Cho and P. Kim, *J. Nat. Prod.*, 2013, **76**, 354–367.

58 B. Krivogorsky, A. C. Nelson, K. A. Douglas and P. Grundt, *Bioorg. Med. Chem. Lett.*, 2013, **23**, 1032–1035.

59 L. A. Onambele, H. Riepl, R. Fischer, G. Pradel, A. Prokop and M. N. Aminake, *Int. J. Parasitol.: Drugs Drug Resist.*, 2015, **5**, 48–57.

60 J. A. Olson, R. J. Terryn, E. L. Stewart, J. C. Baum and M. J. Novak, *J. Mol. Graphics Modell.*, 2018, **80**, 138–146.

61 P. I. Deryabin, T. V. Moskovkina, L. S. Shevchenko and A. I. Kalinovskii, *Russ. J. Org. Chem.*, 2017, **53**, 418–422.

62 Y. N. Hao, J. C. Guo, Z. W. Wang, Y. X. Liu, Y. Q. Li, D. J. Ma and Q. M. Wang, *J. Agric. Food Chem.*, 2020, **68**, 5586–5595.

63 M. Beyrati and A. Hasaninejad, *Tetrahedron Lett.*, 2017, **58**, 1947–1951.

64 D. J. Ramón and M. Yus, *Angew. Chem., Int. Ed.*, 2005, **44**, 1602–1634.

65 C. de Graaff, E. Ruijter and R. V. A. Orru, *Chem. Soc. Rev.*, 2012, **41**, 3969–4009.

66 T. Ahmadi, G. Mohammadi Ziarani, P. Gholamzadeh and H. Mollabagher, *Tetrahedron: Asymmetry*, 2017, **28**, 708–724.

67 D. Zhang and W. Hu, *Chem. Rec.*, 2017, **17**, 739–753.

68 W. H. Brooks, W. C. Guida and K. G. Daniel, *Curr. Top. Med. Chem.*, 2011, **11**, 760–770.

69 H. Alkadi and R. Jbeily, *Infect. Disord.: Drug Targets*, 2018, **18**, 88–95.

70 A. Calcaterra and I. D'Acquarica, *J. Pharm. Biomed. Anal.*, 2018, **147**, 323–340.

71 A. Kumar, V. D. Tripathi and P. Kumar, *Green Chem.*, 2011, **13**, 51–54.

72 A. Ogawa and D. P. Curran, *J. Org. Chem.*, 1997, **62**, 450–451.

73 R. Frauenlob, C. García, G. A. Bradshaw, H. M. Burke and E. Bergin, *J. Org. Chem.*, 2012, **77**, 4445–4449.

74 Y. Li and M.-H. Xu, *Org. Lett.*, 2012, **14**, 2062–2065.

75 S. Lou and S. E. Schaus, *J. Am. Chem. Soc.*, 2008, **130**, 6922–6923.

76 Y. Jiang and S. E. Schaus, *Angew. Chem., Int. Ed.*, 2017, **56**, 1544–1548.

77 M. Carmen Carreño, G. Hernández-Torres, M. Ribagorda and A. Urbano, *Chem. Commun.*, 2009, 6129–6144, DOI: 10.1039/B908043K,.

78 W.-Y. Han, Z.-J. Wu, X.-M. Zhang and W.-C. Yuan, *Org. Lett.*, 2012, **14**, 976–979.

79 W.-Y. Han, J. Zuo, X.-M. Zhang and W.-C. Yuan, *Tetrahedron*, 2013, **69**, 537–541.

80 G. Bocci, E. Carosati, P. Vayer, A. Arrault, S. Lozano and G. Cruciani, *Sci. Rep.*, 2017, **7**, 6359.

81 J. Dong, N.-N. Wang, Z.-J. Yao, L. Zhang, Y. Cheng, D. Ouyang, A.-P. Lu and D.-S. Cao, *J. Cheminf.*, 2018, **10**, 29.

82 A. Lauria, S. Mannino, C. Gentile, G. Mannino, A. Martorana and D. Peri, *Bioinformatics*, 2020, **36**, 1562–1569.

83 A. Daina, O. Michielin and V. Zoete, *Sci. Rep.*, 2017, **7**, 42717.

84 C. A. Lipinski, F. Lombardo, B. W. Dominy and P. J. Feeney, *Adv. Drug Delivery Rev.*, 1997, **23**, 3–25.

85 C. A. Lipinski, *Drug Discovery Today: Technol.*, 2004, **1**, 337–341.

86 A. K. Ghose, V. N. Viswanadhan and J. J. Wendoloski, *J. Comb. Chem.*, 1999, **1**, 55–68.

87 D. F. Veber, S. R. Johnson, H. Y. Cheng, B. R. Smith, K. W. Ward and K. D. Kopple, *J. Med. Chem.*, 2002, **45**, 2615–2623.

88 W. J. Egan, K. M. Merz Jr and J. J. Baldwin, *J. Med. Chem.*, 2000, **43**, 3867–3877.

89 I. Muegge, S. L. Heald and D. Brittelli, *J. Med. Chem.*, 2001, **44**, 1841–1846.

90 P. Ertl, B. Rohde and P. Selzer, *J. Med. Chem.*, 2000, **43**, 3714–3717.

91 J. Ali, P. Camilleri, M. B. Brown, A. J. Hutt and S. B. Kirton, *J. Chem. Inf. Model.*, 2012, **52**, 420–428.

92 A. Daina and V. Zoete, *ChemMedChem*, 2016, **11**, 1117–1121.

93 S. A. Wildman and G. M. Crippen, *J. Chem. Inf. Comput. Sci.*, 1999, **39**, 868–873.

94 J. B. Baell and G. A. Holloway, *J. Med. Chem.*, 2010, **53**, 2719–2740.

95 J. B. Baell and J. W. M. Nissink, *ACS Chem. Biol.*, 2018, **13**, 36–44.

96 G. Roman, *Eur. J. Med. Chem.*, 2015, **89**, 743–816.

97 J. Trigo, V. Subbiah, B. Besse, V. Moreno, R. López, M. A. Sala, S. Peters, S. Ponce, C. Fernández, V. Alfaro, J. Gómez, C. Kahatt, A. Zeaiter, K. Zaman, V. Boni, J. Arrondeau, M. Martínez, J.-P. Delord, A. Awada, R. Kristeleit, M. E. Olmedo, L. Wannesson, J. Valdivia, M. J. Rubio, A. Anton, J. Sarantopoulos, S. P. Chawla, J. Mosquera-Martinez, M. D'Arcangelo, A. Santoro, V. M. Villalobos, J. Sands and L. Paz-Ares, *Lancet Oncol.*, 2020, **21**, 645–654.

98 FDA, FDA grants accelerated approval to lurbinectedin for metastatic small cell lung cancer, (accessed 09/02/2021, 2021).

99 E. Gilberg, D. Stumpfe and J. Bajorath, *RSC Adv.*, 2017, **7**, 35638–35647.

100 CLSI. Clinical and Laboratory Standard Institute, Reference Method for Dilution Antimicrobial Susceptibility Tests. Wayne, PA. Clin. Lab. Stand. Inst. 28. CLSI Document M07-A8 for bacteria, M27-A3 for yeasts and M38–A2 for filamentous fungi.

101 N. M. Martinez-Rossi, T. A. Bitencourt, N. T. A. Peres, E. A. S. Lang, E. V. Gomes, N. R. Quaresemin, M. P. Martins, L. Lopes and A. Rossi, *Front. Microbiol.*, 2018, **9**, 1108.

102 S. Gnat, D. Łagowski and A. Nowakiewicz, *J. Appl. Microbiol.*, 2020, **129**, 212–232.

103 W. L. F. Amarego and D. D. Perrin, in *Purification of Laboratory Chemicals*, Butterworth Heinemann, Oxford, UK, 4th edn, 1996.

104 (a) A. Kumar, V. D. Tripathi and P. Kumar, *Green Chem.*, 2011, **13**, 51–54; (b) L. A. Onambele, H. Riepl, R. Fischer, G. Pradel, A. Prokop and M. N. Aminake, *Int. J. Parasitol.: Drugs Drug Resist.*, 2015, **5**, 4–57.